

(NASA-CR-177476) MINIMUM-COMPLEXITY
HELICOPTER SIMULATION MATH MODEL Final
Contractor Report, Jul. 1985 - Jul. 1987
(Paludyne Systems) 102 p CSCI 01C

N88-25819

G3/08 Unclass
0157133

MINIMUM-COMPLEXITY HELICOPTER SIMULATION MATH MODEL

Robert K. Heffley
Marc A. Mnich

11 25
0157133

Contract NAS2-11665
April 1988



MINIMUM-COMPLEXITY HELICOPTER SIMULATION MATH MODEL

Robert K. Heffley
Marc A. Mnich
Manudyne Systems, Inc.
Los Altos, California

Prepared for
Aeroflightdynamics Directorate
U.S. Army Research and Technology
Activity (AVSCOM)
under Contract NAS2-11665

April 1988

NASA

National Aeronautics and
Space Administration

Ames Research Center
Moffett Field, California 94035

Aeroflightdynamics
Directorate
Moffett Field,
California 94035



ABSTRACT

An example of a minimal complexity simulation helicopter math model is presented. Motivating factors are the computational delays, cost, and inflexibility of the very sophisticated math models now in common use. A helicopter model form is given which addresses each of these factors and provides better engineering understanding of the specific handling qualities features which are apparent to the simulator pilot. The technical approach begins with specification of features which are to be modeled followed by a build-up of individual vehicle components and definition of equations. Model matching and estimation procedures are given which enable the modeling of specific helicopters from basic data sources such as flight manuals. Checkout procedures are given which provide for total model validation. A number of possible model extensions and refinements are discussed. Math model computer programs are defined and listed.

FOREWORD

This report was prepared by Manudyne Systems, Inc., for the U. S. Army Aeroflightdynamics Laboratory located at Ames Research Center. The Contract Technical Monitors were Ms. Michelle M. Eshow and Mr. Christopher L. Blanken.

The Manudyne project engineer was Mr. Robert K. Heffley and the math model development effort was conducted by Mr. Marc A. Mnich.

TABLE OF CONTENTS

I.	Introduction	1
A.	Background	1
	1. Computational Delays	2
	2. Cost of Resources	3
	3. Inflexibility	4
	4. Indirectness of Cause and Effect Relationships ..	4
B.	Merits of Considering a Simple Math Model Form	5
	1. Cost	5
	2. Quality	5
	3. Engineering Understanding	5
C.	Model Attributes to be Considered	6
	1. Simulator Application	6
	2. Handling Qualities Application	6
	3. Full Flight Envelope Operation	6
	4. Modularity	7
	5. Microcomputer Adaptability	7
D.	Report Organization	7
	1. Modeling Approach	7
	2. Matching and Estimating Procedures	7
	3. Checkout Procedures	8
	4. Model Extensions and Refinements	8
II.	Technical Approach	9
A.	Specification of Desired Math Model Features	9
	1. First-Order Flapping	10
	2. Main Rotor Induced-Velocity Computation	10
	3. Rigid-Body Degrees of Freedom	10
	4. Power Requirements Over Flight Envelope	11
	5. Rearward and Sideward Flight	11
	6. Hover Dynamic Modes	11
	7. Forward-Flight Dynamic Modes	11
	8. Correct Transition from Hover to Forward Flight ..	12
	9. Effects of Rotor RPM Variation	12
	10. Cross Coupling	12
	11. Correct Power-Off Glide	12
B.	Component Build-Up	13
	1. Main rotor	16
	2. Fuselage	17
	3. Tail Rotor	17
	4. Horizontal Tail	17
	5. Wing	18
	6. Vertical Tail	18
C.	Definition of Model Equations	18
	1. Main Rotor Thrust and Induced Velocity	18
	2. Tail Rotor Thrust and Induced-Velocity	20

3.	Fuselage Geometry and Drag	20
4.	Horizontal Tail Geometry and Lift	21
5.	Wing Geometry and Lift	22
6.	Vertical Tail Geometry and Lift	23
7.	Total Power Required	24
8.	Summation of Force and Moment Equations	24
9.	Integration and Axis Transformation	25
10.	Summary of Model Parameters	26
III.	Model Matching and Estimation Procedures	28
A.	Mass, Loading, and Geometry Data	28
1.	Geometric Data	28
2.	Mass and Loading Data	30
B.	Propulsion Data	33
C.	Rotor Data	36
D.	Aerodynamic Features	36
E.	Hover Performance	39
F.	Forward Flight Data	41
IV.	Checkout Procedures	46
A.	General	46
B.	Discussion of Checkout Procedure Elements	46
1.	Independent Operating Program	46
2.	Trim Point Verification	47
3.	State Transition Verification	48
4.	Time History Overlays	51
5.	Dominant Response Identification	53
V.	Model Extensions and Refinements	54
A.	Flight Control System	54
B.	Engine-Governor	54
C.	Ground Effect	54
D.	Dynamic Inflow	55
E.	Higher-Order Flapping, Coning, and Lead-Lag Dynamics	55
References	56
Appendix A.	Listing Of Dynamics Subroutine	A-1
Appendix B.	Definition of Dynamics Subroutine Symbols	B-1
Appendix C.	Input Data	C-1
Appendix D.	Agusta A-109 Math Model Example	D-1

LIST OF FIGURES

Figure 1. Tradeoff of Math Model Cost with User Utility. . . .	2
Figure 2. Basic Helicopter Math Model Components.	14
Figure 3. Main Rotor Thrust and Induced-Velocity Block Diagram.	18
Figure 4. Basis for Geometric Data.	29
Figure 5. Basis for Loading Data.	31
Figure 6. Basis for Torque (Power) Limits.	35
Figure 7. Basis for Initial Estimates of Aerodynamic Parameters.	38
Figure 8. Basis for Hover Power Required.	40
Figure 9. Basis for Forward Flight Speeds and Power Required.	42
Figure 10. Basis for Max Rate of Climb Speed and Power Required.	43
Figure 11. Basis for Max Glide Speed and Descent Angle.	44
Figure 12. Sample of Trim Point Printout.	47
Figure 13. Examples of Time Histories to be Used for Overlays.	52

LIST OF TABLES

Table 1.	Desired Features	9
Table 2.	Single-Rotor Helicopter Coupling Sources.	13
Table 3.	Details of Component Build-Up.	15
Table 4.	Basis for Inertial Data	32
Table 5.	Basis for Propulsion System Data.	34
Table 6.	Assumed Breakdown of Power Absorbtion.	34
Table 7.	Sample of State Transition Checks.	49

MINIMUM-COMPLEXITY HELICOPTER SIMULATION MATH MODEL PROGRAM

I. Introduction

A. Background

The past decade has seen a trend toward increasingly complex simulator math models. Part of this has been a result of more flight control system sophistication and attention toward a number of aerodynamic factors, including interactive aerodynamics and aeroelastic effects. Another reason is the availability of large, high speed mainframe and mini-computers. Some simulation uses such as aircraft design or failure analysis do justify attention to detail. Other applications, including may handling qualities evaluations, may be better served with lesser sophistication. Since high complexity also carries the burden of high cost of engineering labor and computer facilities, one should exercise judgment in math model design. Engineering management should be concerned when there is a neglect to determine precisely the degree of complexity really needed for a given application.

The purpose of this report is first to discuss the reasons for striving for minimal math model complexity and second to offer an example of a reasonably useful and credible helicopter math model form offering real economy in terms of development and computational requirements. Evaluation of handling qualities is the main application under consideration here, but the same kinds of factors would apply to other simulation uses.

The question being considered is really one of math model value versus cost. The value must ultimately be expressed as the utility of a math model to provide necessary features which can be perceived and used by the simulator pilot. One should expect that, as a function of complexity, this model utility approaches a fairly flat asymptote with some reasonable level of complexity. The other side of the coin is the cost of math model development and checkout, also a function of complexity. Unfortunately this function can be expected to increase exponentially. These contrasting relationships are sketched in Figure 1. The obvious question for the simulator user is at what level of model complexity do these two cost/value curves cross. That is, what is the point of diminishing returns on model complexity?

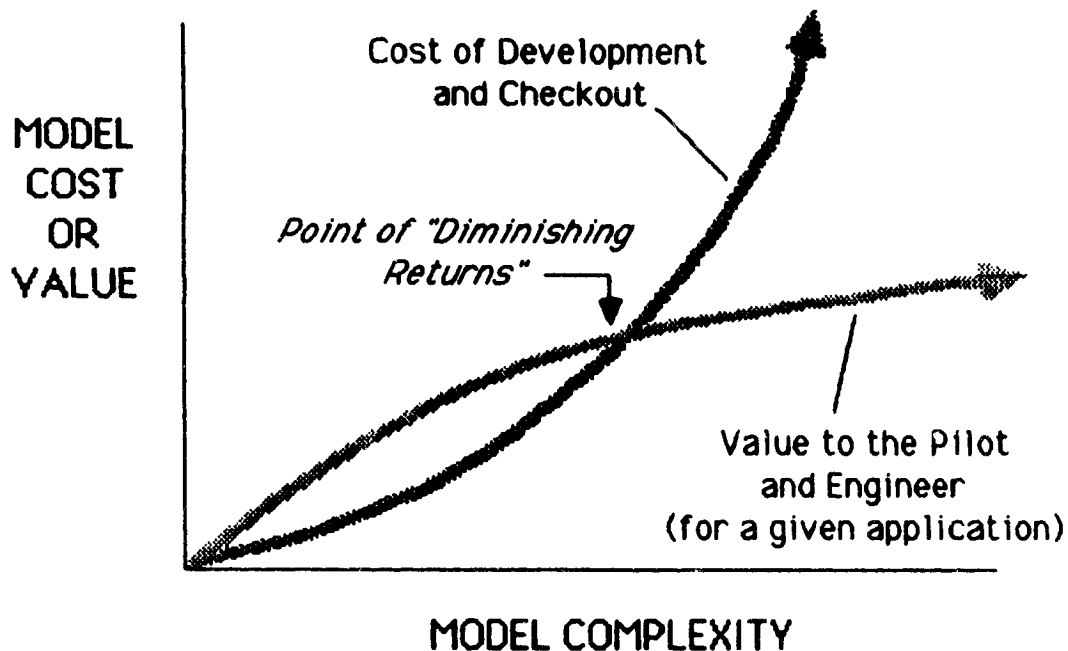


Figure 1. Tradeoff of Math Model Cost with User Utility.

Experience typical of that described in References 1 and 2 has taught that math model complexity alone does not automatically provide effectiveness in handling qualities simulations. Rather, there can be distracting factors which work counter to simulation objectives. Ultimately, limited resources prevent one from realizing the full potential of an overly complex simulator math model. Other limitations can be a lack of flexibility in modeling and restricted clarity in the cause and effect relationships between model parameters and features. These shortcomings raise questions about the value of complexity in helicopter math models and are a motivation to consider simpler models.

The following are some of the undesirable effects of excessive math model complexity.

1. Computational Delays

Computational lag and delay is a particularly important problem resulting from model complexity. As complexity grows, computational delay associated with the math model code increases and, in turn, compounds overall visual system delay. Computer speed is limited by the hardware and software system being used and cannot be easily changed.

The result of the delays imposed is reduced fidelity. NASA Ames, for example, employs both a Xerox Sigma 8 and CDC 7600 for their Vertical Motion Simulator (VMS). Using the currently implemented ARMCOP helicopter math model (Reference 3) and the faster of the two computers (CDC 7600), the computational delay is about 25 milliseconds. The Sigma may require 60 to 75 milliseconds to cycle. The former speed is acceptable for some math model solutions but visual system digital delay of about 100 milliseconds can still remain. Although the impact of this amount of delay has been minimized at Ames (using methods such as those presented in Reference 4), more software complexity has been added to correct a problem originally caused by complexity. It would seem that this is not as cheap and effective as preventing the problem by simplifying the model in the first place.

2. Cost of Resources

As model complexity and the amount of computer code grows, so do the time and effort required to implement, check, and debug the code. The time available to do these is often limited and can affect overall math model fidelity if neglected. ARMCOP, for example, has several thousand lines of code. In checking and debugging code in large programs, a certain number of errors will go undetected, and the more code there is, the more likely errors will persist.

In addition to checking and debugging code, there is the task of determining model parameters needed to represent a specific aircraft. The time and effort required to thoroughly validate the model against the real aircraft can be an expensive part of any simulation. Math models employing look-up tables can have hundreds of parameters which need to be set and confirmed. Since some of these values are estimates, an iterative process may be required. Limits on time and manpower may restrict this process and the fidelity of the model.

Validation of the math model equations (as opposed to math model code) is also a process which may require iteration as the model is changed. It is possible that errors in the math model will exist even as the model is being used in simulation. Again, the number of errors which exist and the time required to fix them is a function of the complexity of the model. Time and manpower restrictions will limit the ability of the users to find and correct these errors and thus degrade the fidelity of the model. In order to guarantee that a model is completely correct, all parts of the model must be exercised. Lookup tables, for example, require that all numbers in the table be verified as well as checked for discontinuities. All equations in the model need to be checked to ensure they are theoretically sound. With complex code, it is unlikely that all of the model will be checked as thoroughly as necessary and errors can persist in actively used models for long periods of time before they are ever noticed or corrected.

ARMCOP, for example, still exhibits a problem affecting maneuvering flight even though the model has seen wide use. This involves a large speed loss during sustained turns. Although detected, this problem has not been corrected because of insufficient engineering labor resources. Rather problems are "patched up" with flight control system modifications (in this case a turn-coordinator). Again, complexity is added to fix a problem itself arising from model complexity.

3. Inflexibility

There is an inherent tradeoff between complexity and flexibility in models of dynamic systems. As more components or features are added to a model, it becomes increasingly difficult and expensive to perform other modifications. One measure of the flexibility of a model is its adaptability to new computer systems and languages or to changes in the code. Large sets of code are limited to large computer systems. ARMCOP, for example, requires the use of a mainframe system. In order to work with the model, one must have access to such facilities.

Once code has been implemented on a machine, it must be checked and debugged. Modifications for debugging may require recompilation. Most such changes are made before the code is used for actual simulation, but it is possible that they will be made during a simulation. Even simple model changes can consume enough time to hamper simulator productivity. It is not uncommon for a software modification, followed by a graphical check, to require 20 or 30 minutes of simulator occupancy time.

The ability to add, remove, or modify efficiently the dynamic characteristics of a model is another measure of its flexibility. It may be desirable, for example, to have a helicopter simulation without rotor cross coupling. A model such as ARMCOP, in which cross coupling is inherent, does not allow easy removal of this feature. In fact, coupling might be "removed" by adding control system functions to suppress the coupling, thus further increasing the complexity of the model. The emphasis in modeling should be on efficiency while maintaining adequate fidelity.

4. Indirectness of Cause and Effect Relationships

The ability to see the relationship between model parameters and model response features is decreased with complexity. This relationship is important to handling qualities simulation work for two reasons. First, is the need to easily make changes in model features. Second is the need to trace errors which appear in the response modes of the model. These are fundamental to working effectively with the model. In order to modify response features, one must know what parameters are responsible for those features and how to change them. In any math model, individual parameters tend to become coupled to many

features at once making it difficult to change such features independently. The more complicated that math model, the more impossible is it to manage individual model response features.

B. Merits of Considering a Simple Math Model Form

Turning from the above list of difficulties issuing from model complexity, consider some of the direct, positive aspects of considering a simple math model form at the outset.

It would appear that there are compelling benefits for general reductions in the levels of complexity exemplified by math models such as ARMCOP and GENHEL (Reference 5). This leads us to consider ways to find a compromise between math model complexity and simulator utility. At one extreme are the highly complex models which attempt to achieve effectiveness through high computational fidelity. As mentioned, these models encounter practical limits which not only hamper fidelity but also reduce their flexibility and clarity between parameters and features. At the other extreme are models such as the linearized stability derivative form which are easier to manage but which may lack fidelity or be restricted to a small operating envelope.

The merits of a "compromise" model form would thus be cost and quality benefits derived from the achievement of specific fidelity features through minimal software program instructions.

1. Cost

The cost benefits will accrue through minimizing labor required to quantify and checkout the math model implementation. Development of even modest math models typically involve more than one man year of labor. If this process can be shortened to less than one man-month, the period envisioned for the proposed form, then great savings clearly can be realized.

Simulator math model software checkout can also require substantial effort. However, this is often simply limited by time available and the job might not actually be completed prior to simulator use. Again the aim is to realize greatly reduced checkout time through software reduction and to make a comprehensive checkout feasible within a short period of time.

2. Quality

The quality benefits come from confidence that specific features needed for effective simulation are represented and that they are correct. Here quality arises from the fact that implementation and checkout tasks which should be done are, in fact, done. In a real sense, quality follows the degree of manageability afforded by the simulator software.

3. Engineering Understanding

One of the most important benefits to be derived from a minimum-complexity math model is in the potential for more clearly understanding cause and effect relationships. For example, if a particular kind and amount of cross-coupling is desired, then how does one achieve it through adjustment of math model parameters? It is possible by having a close, easy-to-follow connection between the physical component representation and the resulting physical response features.

An important value of engineering understanding is the ability to make model adjustments or refinements in a direct, efficient a manner as is possible for a physical helicopter model.

C. Model Attributes to be Considered

1. Simulator Application

It should be stressed that in this case the goal of the math model is to be an effective tool for simulation. Model fidelity alone is not the solution to simulator effectiveness. Rather, it is the ability of the model to produce the desired results and insights for the given application. Besides having adequate fidelity, the model must also be affordable, manageable, easily modified and checked, and have a reasonably clear cause and effect relationship between parameters and response features (at least those perceivable by the pilot).

2. Handling Qualities Application

Thus we are motivated to turn to a simple model with these qualities for helicopter handling qualities simulation which can be a more effective tool than existing models. Specifically, the purpose here is to propose a minimum-complexity model format suitable for helicopter handling qualities simulation.

It should be remembered that many handling qualities investigations involve examination of fairly crude and simple parameters such as time constants, damping ratios, or static gains. Furthermore the precision with which evaluation pilots can perceive such changes often can be disappointing to the engineer. Thus it is not reasonable to expect that high math model resolution is really crucial. If a pilot cannot actually observe or be influenced by certain math model effects then those effects should probably be considered as excessive complication. (Unfortunately, there is presently little quantification of just how sensitive a pilot is to various effects, and this is a potential application of a minimum-complexity math model.)

3. Full Flight Envelope Operation

The model should be nonlinear and apply to the full operating range of a real helicopter including rearward as well as forward flight, sideward flight, hover, and transition from hover to forward flight. The model should include at least

first-order flapping degrees of freedom and all rigid body degrees of freedom. The higher-order flapping modes and any structural modes beyond the frequency range of interest for handling qualities should not be included unless high-gain flight control systems are involved.

4. Modularity

The form of the model will be modular. This will allow the flexibility of adding alternative rotor models, if desired, as well as other lifting surfaces. Any combination of components can be combined including models of pilots and control systems making the model adaptable to a variety of helicopters and subsystems. The full utility of the proposed model format will become apparent as the structure of the model is described in more detail.

5. Microcomputer Adaptability

The math model form will be compatible with microcomputer use, at least on a non-real-time basis. It has been found that math model development and checkout can be done to a large extent on small, inexpensive desktop microcomputers. This of course demands that the software be reasonably compact.

D. Report Organization

The presentation which follows consists of four parts: (i) approach to modeling, (ii) matching and estimation procedures, (iii) checkout procedures, and (iv) extensions and modifications of the model. In addition various detailed information is contained in appendices.

1. Modeling Approach

In the first section, the modeling approach is described in order to establish the theoretical foundation for the model. This is useful for understanding, modifying or extending the model and for its effective use as a simulator tool. In addition, a description of the features and components of this specific model is given. The model is used to represent a Bell AH-1S Cobra. All parameters and variables from this aircraft are provided here along with the actual code. The sample version shows the extent of the code in terms of number of parameters, number of lines of code, number of computations, etc. and can be compared to an ARMCOF version of the same aircraft.

2. Matching and Estimating Procedures

In the next section, the matching and estimating procedures used to obtain model parameters are described. The sample version of the AH-1S is used as a specific example. The model is then exercised and the estimated parameters varied in order to tune the model to fit performance data.

3. Checkout Procedures

The third section describes several methods of checking the math model code. The size of the model and the modular format are conducive to efficient checking. Methods are then presented for verifying the math model equations and are illustrated using the sample version.

4. Model Extensions and Refinements

Finally, in the last section, possibilities for extending or modifying the model are introduced to demonstrate the flexibility of the model format. The potential for a much improved level of simulation effectiveness using these extensions and modifications is revealed and explained in terms of the approach taken to the modeling process.

II. Technical Approach

A. Specification of Desired Math Model Features

The approach to modeling will begin with a list of desired features. This list will serve as a specification upon which to formulate a minimum-complexity model containing only those components and equations directly responsible for the desired features. The model will be customized to the problem being studied.

We shall assume that the model is intended for handling qualities simulation and that the features to be included in the model should be features which are observable or needed by a pilot. It should be assumed that the model will be operated over a specified flight envelope and controlled by a given flight control configuration. This sets limits on speed, acceleration, and frequency response. The features to be included by the following example are listed in Table 1. Of course these are subject to change depending upon the application.

Table 1. Desired Features

-
1. First-order flapping dynamics for main rotor (coupled or uncoupled).
 2. Main rotor induced velocity computation.
 3. All rigid-body degrees of freedom.
 4. Realistic power requirements over desired flight envelope.
 5. Rearward and sideward flight without computational singularities.
 6. Hover dynamic modes:
 - longitudinal and lateral hover cubics
 - rotor-body coupling with flapping
 7. Forward flight dynamic modes:
 - short period and phugoid
 - roll mode and Dutch roll
 - rotor-body coupling with flapping
 8. Dihedral effect.
 9. Correct transition from hover to forward flight.
 10. Potential for rotor RPM variation.
 11. Correct power-off glide for min R/D and max glide.

1. First-Order Flapping

It has been shown in Reference 6 that rotor flapping can couple with rigid-body modes in regions which affect handling qualities. This occurs in the lower frequency or "regressing flapping" modes. However, this effect can be modeled with a first-order flapping equation in the pitch and roll axes.

The time constant involved in the regressing flapping mode is directly proportional to the product of rotor angular velocity and Lock number. Thus only the commonly available rotor mass and geometric parameters are needed.

The actual flapping response is modified by coupling with the fuselage at the hub restraint. Since this involves the classical rigid body modal response, it is discussed further under items 6 and 7 below.

The feature of flapping which is most important to a pilot-in-the-loop simulation is the apparent control lag following cyclic input. This lag is in effect the time required to precess the tip path plane to a new orientation. A typical value for the effective lag is about 0.1 sec--significant because it is comparable to the pilot's own neuromuscular lag.

2. Main Rotor Induced-Velocity Computation

A particularly important feature of a helicopter is the relationship among thrust, power, and airspeed. This relationship arises from the induced-velocity of air passing through the rotor disc.

There are a number of complicating factors, but, to a first-order approximation, induced-velocity effects can be modeled with a classical momentum theory model wherein thrust and induced-velocity interact in an aerodynamic feedback loop. Computation is complicated, however, because this feedback is highly nonlinear.

Another aspect of the induced-velocity is its effect on adjacent surfaces. The rotor induced-velocity field impinges on the wing, horizontal tail, and fuselage and varies with airspeed and flight path direction.

3. Rigid-Body Degrees of Freedom

Normally, six rigid-body degrees of freedom are needed for useful manned simulation. Pilot workload arises from constant attention to roll, pitch, and yaw as well as translation fore-and-aft, to the side, and vertically. Only under special conditions might one desire to eliminate one of these via, for example, the assumption of perfectly coordinated forward flight.

4. Power Requirements Over Flight Envelope

A common source of real aircraft data appropriate for verifying a math model is performance data in terms of power required for various trim conditions. The power or torque required is immediately obvious and important to a pilot and varies substantially from hover through transition and finally in forward flight.

Power requirements can be easily computed once main and tail rotor induced velocities are established.

5. Rearward and Sideward Flight

In a full-flight-envelope model involving circulation lifting surfaces, computational singularities can exist, depending upon the model form used. These singularities come from trigonometric functions for angle of attack, sideslip, etc., but are avoided in this model by using a quadratic lift coefficient method. For this technique, forces for lifting surfaces are computed using quadratic coefficients multiplied by the squares of velocity components so that negative velocities cannot cause singularities. No explicit computation of angle of attack or sideslip is needed and, indeed, should be completely avoided.

6. Hover Dynamic Modes

Hovering flight is characterized by similar dynamics in each the pitch and roll axes, including sets of high and low frequency response modes. In addition, the yaw axis contains a predominant yaw damping mode. These dynamics can couple with regressing flapping dynamics. All are apparent to the pilot in operating the aircraft whether trimming, maneuvering, or flying unattended.

Pitch and roll are classically described by the "hover cubic," but this generally neglects coupling with the rotor which can be important. This is easily computed, however, through inclusion of the flapping dynamics as described earlier.

The phugoid mode for hover results from the combination of dihedral and gravity force. Effective dihedral is particularly apparent in unaggressive sideward flight because the pilot must continually add lateral control as sideward velocity increases.

7. Forward-Flight Dynamic Modes

In forward flight, the dominant rigid body dynamics of a helicopter resemble those of a conventional fixed-wing airplane and include short-period, phugoid, dutch roll, and spiral modes. There is also likely to be significant coupling with flapping dynamics.

8. Correct Transition from Hover to Forward Flight

Transition effects are an important part of the piloting task when accelerating from hover into the forward flight region.

These effects are a combined result of a "dihedral effect" in the x-axis and the varying rotor downwash effect on the horizontal tail.

9. Effects of Rotor RPM Variation

Rotor RPM can affect helicopter dynamics in a number of ways, including thrust, flapping response, and heave damping.

The effects of rotor speed variation are tied, however, to the rotor-engine-governor combination. For a number of applications it may be sufficient to assume a constant rotor RPM. This will be done here.

10. Cross Coupling

A variety of cross coupling effects can be present in helicopters. Some of these such as collective-to-yaw coupling are easy-to-see, first-order phenomena. These are generally inherent in the basic dynamics if reasonable first-principles thrust and rotor models are used.

Other coupling effects may be more subtle or less predictable and should be added only where needed or desired by the simulator user. These can be inserted directly in the equations of motion as coupling terms arising from both states and controls. One should distinguish among coupling due to (i) rotor hub moments, (ii) flapping dynamics, and (iii) dihedral effects.

Cross-coupling occurs naturally when coupled rotor and hub-moment expressions are included. However, these may not suffice in matching actual cross-coupling observed in a particular design. One approach is to begin with decoupled equations then systematically add terms which provide a suitable match. (This is demonstrated in the A109 example in Appendix D.

A useful guide to cross-coupling sources is borrowed from Reference 7 and shown below in Table 2.

11. Correct Power-Off Glide

Helicopters, like fixed-wing aircraft, need to exhibit reasonable performance when power is reduced. This can be a highly complex issue if ring vortex rotor states are included. However, many handling qualities investigations can be conducted using only the normal thrust model described above but tailoring the full-down collective pitch and aerodynamic drag to yield realistic forward-velocity autorotative glide characteristics.

Table 2. Single-Rotor Helicopter Coupling Sources.

Response Input Axis	Pitch	Roll	Yaw	Climb/Descent
<i>Longitudinal Stick</i>	Prime	(1) lateral flapping due to longitudinal stick (2) lateral flapping due to pitch rate (3) lateral flapping due to load factor	Negligible	Desired for vertical flight path control in forward flight
<i>Lateral Stick</i>	(1) longitudinal flapping due to lateral stick (2) longitudinal flapping due to roll rate	Prime	(1) Undesired in hover, caused by directional stability (2) Desired for turn coordination and heading control in forward flight	Descent with bank angle at fixed power
<i>Rudder</i>	Negligible	(1) Roll due to tail rotor thrust (2) Roll due to sideslip	Prime (hover)	Undesired due to power changes in hover
<i>Collective</i>	(1) Transient longitudinal flapping with load factor (2) Steady longitudinal flapping due to climb/descent in forward flight caused by rotor flapping (3) Pitch due to changes in horizontal tail lift	(1) Transient lateral flapping with load factor (2) Steady lateral flapping with climb and descent (3) Sideslip induced by power change causes roll due to dihedral	Power change varies requirement for tail rotor thrust	Prime

(Borrowed from Blake and Alansky, AHS Forum, 1975)

B. Component Build-Up

With a specification of desired features, essential model components can then be chosen. These components contain the mechanisms which provide forces and moments, power dissipation, stability and control, and rotor dynamics.

The six components are considered necessary to provide all of the above response features are shown in Figure 3. Table 3 lists these components along with the physical features of each component and the resulting response features. In effect, this is a list of qualitative model requirements which form a starting point for detailed model design. The components and their physical elements are described and discussed individually below.

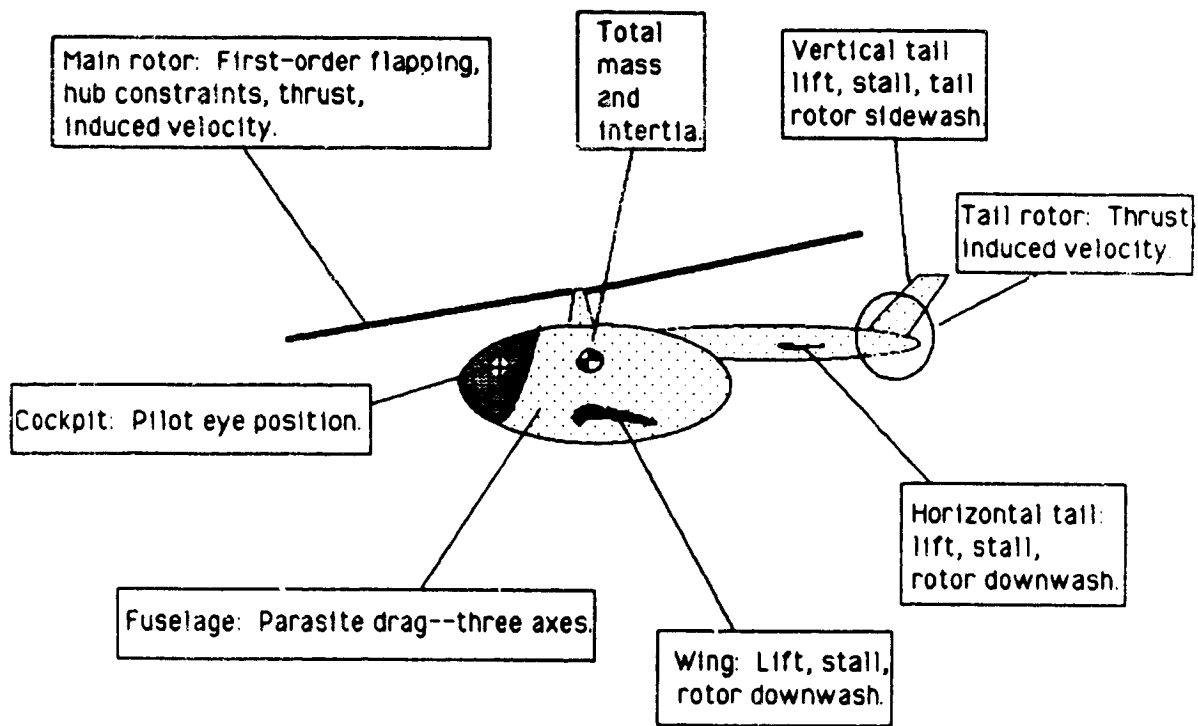


Figure 2. Basic Helicopter Math Model Components.

Table 3. Details of Component Build-Up.

Components	Physical features	Response features
1.) Main rotor:	Thrust Torque Induced velocity Tip path plane lag Induced power Profile power No off-axis flapping stiffness Decoupled TPP dynamics Constant RPM	1st order flapping Power required Trim Phugoid Short period Dihedral Pitch mode Roll mode Min x-coupling Power off glide
2.) Fuselage:	Mass at C.G. Moments of inertia Parasite power Cross products of inertia = 0	Trim Power required Min x-coupling Power off glide
3.) Tail rotor:	Thrust Torque Induced velocity Induced power Profile power	Trim Power required Roll mode
4.) Horizontal tail:	Lift / Stall Exposure to main rotor induced vel.	Short period Trim Pitch mode Power required
5.) Wing:	Lift / Stall Induced drag Induced power Exposure to main rotor induced vel.	Trim Power required
6.) Vertical tail:	Lift / Stall	Dutch roll Roll mode

1. Main rotor

The primary component of this model is the main rotor. It is the main feature responsible for producing characteristics unique to a helicopter, in particular, a vertical thrust vector and an induced-velocity field. Other key features include rotor torque, dihedral effect, flapping stiffness (rate damping), and flapping dynamics (tip-path-plane lag).

The basis for the model used here is primarily the autogyro theory presented by Glauert in Reference 8 and extended by Lock in Reference 9. The higher order flapping dynamics as defined by Chen in Reference 6 are simplified according to the first-order model developed by Curtiss and presented in References 1 and 2.

Thrust and induced velocity are computed assuming a uniform flow distribution. As described earlier, the tip-path-plane orientation (flapping angles) are modeled as simple first order lags giving the main rotor the qualities of a force actuator with a lag. The tip-path-plane dynamics can be extended using either a coupled first-order model or a coupled second-order model based on simplification of Chen's rotor equations in Reference 5.

The main rotor model contributes largely to the power requirement feature of the model. In hover, nearly 80% of total power is absorbed by the main rotor, and, in forward flight, it is as much as 60%. In hover, rotor downwash on the fuselage also contributes to power losses.

Tip path plane and hub moment equations were rederived in a body-fixed axis system from the equations in References 3 and 6. This was done in order to avoid the real-time hover simulation problems which can arise from large instantaneous changes in the wind-axis angles for small changes in body-axis translational velocities.

It is suggested that two major components of cross coupling be avoided until the detailed model matching process is underway. One of these is the off-axis hub moments due to flapping (L_{a1} and M_{b1}), and the second is the off-axis coupling in the tip path plane dynamics. It has been found that including these higher-order effects in a simple model does not automatically produce a high quality match to flight data.

The dihedral effect is included through the variables db_1/dv and da_1/du which appear in the first order flapping equations. Values can be computed using first-principles factors consisting of thrust coefficient and tip velocity. The dihedral feature is responsible for the phugoid-like modes in hover and forward flight.

The portion of L_{b1} and M_{a1} due to both hinge offset and rotor spring stiffness are included in a separate parameter, $dL.dA1$. Thus, the total flapping stiffness can be directly varied through this one parameter.

Pitch and roll mode time constants are a function of both body pitch and roll damping and rotor tip path plane lag. Control over these time constants can thus be exercised through the flapping lag as well as body aerodynamic damping.

2. Fuselage

The fuselage is represented as a virtual flat plate drag source having three dimensions. The effective aerodynamic center can be located at any position in the body reference frame. It would normally be expected to be near the geometric center.

The fuselage drag model is based on a quadratic aerodynamic form originally found in the hydrodynamics text by Lamb (Reference 10) and used extensively for airship applications by Monk (Reference 11). This form can be easily extended to account for fuselage assymetries, lifting effects, and lift gradients.

The simple fuselage aerodynamic form presented here provides for drag in forward flight which limits maximum airspeed, drag in sideward flight, and rotor downwash impinging on the fuselage. All three of these effects are related to power losses.

3. Tail Rotor

The tail rotor component is modeled in the same manner as the main rotor except that no flapping degree of freedom is included. In effect, only Glauert's equations apply. However thrust, induced-velocity, and power effects are correctly modeled. Normal directional control is provided through the tail rotor collective pitch variation.

4. Horizontal Tail

The horizontal tail is assumed to be primarily a lift producer, thus only the normal force component is modeled. This still provides for computation of drag resulting from induced-lift if that is desired. Finally, the effects of aerodynamic stall are included. The geometric location of the horizontal tail in the rotor flow field is used to obtain the local apparent wind component. The location of the horizontal tail provides effective static stability and elevator control.

As with the fuselage aerodynamics, a basic quadratic form is used. Two terms model the effects of camber and circulation

lift. One additional term and conditional test is included to model the effect of stall.

5. Wing

The wing component follows the same form as the horizontal tail. In addition, the induced drag is computed in order to obtain the related power-required component which can be significant during sustained-g maneuvering.

6. Vertical Tail

The vertical tail is also similar to the horizontal tail except that it experiences the flow field produced by the tail rotor.

C. Definition of Model Equations

Once the various components of the model are defined, the equations for all the components must be expressed in a way which minimizes code and the number of parameters. The following does so according to the order of the computer program.

1. Main Rotor Thrust and Induced Velocity

The computation of thrust and induced velocity is based on a classical momentum theory equation, but with a special recursion scheme which yields a very quick convergence. The block diagram showing the thrust and induced velocity equations is given in Figure 3.

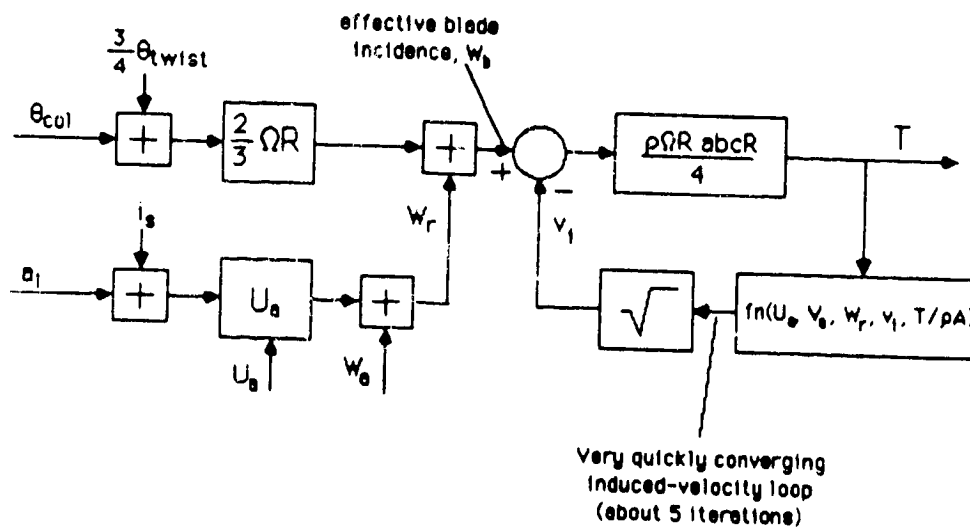


Figure 3. Main Rotor Thrust and Induced-Velocity Block Diagram.

The recursion relationship is based on breaking the thrust-induced velocity loop at the induced-velocity node and iterating on a solution for thrust followed by induced-velocity. This yields a fast convergence with a fixed number of iterations--about 5 is sufficient.

$$T = (W_b - v_i) \cdot \frac{\rho \Omega R abcR}{4}$$

$$v_i^2 = \sqrt{\left(\frac{\hat{v}^2}{2}\right)^2 + \left(\frac{T}{2\rho A}\right)^2} - \frac{\hat{v}^2}{2}$$

where

$$W_r = W_a + (a_1 + i_s) U_a - b_1 V_a$$

$$W_b = W_r + \frac{2}{3} R [\theta_{col} + \frac{3}{4} \theta_{twist}]$$

$$\hat{v}^2 = U_a^2 + V_a^2 + W_r(W_r - 2v_i)$$

$$A = \pi R^2$$

Once induced velocity for the main rotor has been computed, one can compute the longitudinal and lateral dihedral effects of the main rotor which are, in turn, dependent on induced velocity:

$$db_1/dv = da_1/du = \frac{2}{\Omega R} \left(\frac{\partial C_L}{\partial \alpha} + \sqrt{\frac{C_T}{2}} \right)$$

The main rotor parameters needed for these equations are:

d^{mr} , horizontal distance of hub from c. g.

h^{mr} , hub height above the c. g.

R, rotor radius.

abcR, product of lift slope, number of blades, chord, and radius.

θ_{twist} , effective blade twist.

Ω , main rotor angular rate.

2. Tail Rotor Thrust and Induced-Velocity

Thrust and induced velocity for the tail rotor is computed in the same manner as for the main rotor except that no flapping effects are included.

The parameters which define the tail rotor effects are:

d^{tr} , distance of tail rotor from c. g.

h^{tr} , height of tail rotor above c. g.

R^{tr}

$(abcR)^{tr}$, product of lift slope, number of blades, chord, and radius.

Ω^{tr} , tail rotor angular rate.

3. Fuselage Geometry and Drag

Profile drag forces are computed for the fuselage in the x-, y-, and z-axes. These drag forces can constitute a significant portion of the overall power required and thus must be computed prior to main rotor torque. The forces are computed at the center of pressure located at the point (X.FUS, Y.FUS, Z.FUS) relative to the center of gravity.

Fuselage drag forces are computed using a "quadratic aerodynamic form." In this case forces are expressed as a summation of terms formed by the product of translational velocity components in each axis. The constants in each term are the effective flat plate drag.

$$W_a^{fus} \triangleq W_a + v_i \quad \text{local w-velocity}$$

$$X_{aero}^{fus} = \frac{\rho}{2} X_{uu}^{fus} U_a \cdot U_a \quad \text{drag component}$$

$$Y_{aero}^{fus} = \frac{\rho}{2} Y_{vv}^{fus} V_a \cdot V_a \quad \text{side-force component}$$

$$Z_{aero}^{fus} = \frac{\rho}{2} Z_{ww}^{fus} W_a^{fus} \cdot W_a^{fus} \quad \text{downwash component}$$

Moments due to the drag forces relative to the center of gravity are computed.

The parameters required for the fuselage are:

d^{fus} , distance of fuselage a. c. from c. g.

h^{fus} , height of fuselage a. c. from c. g.

X_{uu}^{fus} , effective flat plate drag in x-axis

Y_{vv}^{fus} , effective flat plate drag in y-axis

Z_{ww}^{fus} , effective flat plate drag in z-axis

4. Horizontal Tail Geometry and Lift

The horizontal tail is modeled in terms of a quadratic aerodynamic form for airfoils.

The first step in computing the lift on the horizontal tail is to determine whether the surface is immersed in the rotor downwash field. This will influence the local vertical velocity vector.

The next step is to check for aerodynamic stall by comparing the force computed above with the maximum achievable at the same airspeed.

$$W_0^{ht} \triangleq W_0 + v_i \quad \text{local w-velocity}$$

$$Z_{aero}^{ht} = \frac{\rho}{2} (Z_{uv}^{ht} U_0 U_0 + Z_{uw}^{ht} U_0 W_0^{ht}) \quad \text{normal force}$$

$$> \frac{\rho}{2} Z_{min}^{ht} U_0 U_0 \quad \text{stall condition}$$

Pitching moment due to the horizontal tail is computed based on the location of the aerodynamic center relative to the center of gravity.

The parameters required for horizontal tail effects are:

d^{ht} , distance of horizontal tail from c. g.

h^{ht} , height of horizontal tail from c. g.

z_{uu}^{ht} , aerodynamic camber effect

z_{uw}^{ht} , lift slope effect

z_{min}^{ht} , stall effect

5. Wing Geometry and Lift

The wing is treated in the same manner as the horizontal tail. It is first checked for exposure to main rotor downwash and then for stall. For the wing, induced drag is computed in order to determine the power loss due to this effect. Lift and pitching moment for the wing are also computed.

$W_0^{wng} \triangleq W_0 + v_i$	local w-velocity
$Z_{aero}^{wng} = \frac{\rho}{2} (Z_{uu}^{wng} U_0 U_0 + Z_{uw}^{wng} U_0 W_0^{wng})$	normal force
$> \frac{\rho}{2} Z_{min}^{wng} U_0 U_0$	stall condition

The power due to the induced drag of the wing is computed based on the product of force and velocity in the x-axis.

The parameters required for wing effects are:

d^{wng} , distance of wing from c. g.

h^{wng} , height of wing from c. g.

Z_{uu}^{wng} , aerodynamic camber effect

Z_{uw}^{wng} , lift slope effect

Z_{min}^{wng} , stall effect

6. Vertical Tail Geometry and Lift

The vertical tail is treated the same as the other lifting surfaces except that it is assumed out of main rotor downwash.

$$V_a^{vt} \triangleq V_a + v_i^{tr} \quad \text{local v-velocity}$$

$$Y_{aero}^{vt} = \frac{\rho}{2} (Y_{uu}^{vt} U_a U_a + Y_{uv}^{vt} U_a V_a^{vt}) \quad \text{normal force}$$

$$> \frac{\rho}{2} Y_{min}^{vt} U_a U_a \quad \text{stall condition}$$

The parameters required for vertical tail effects are:

d^{vt} , distance of vertical tail from c. g.

h^{vt} , height of vertical tail from c. g.

Y_{uu}^{vt} , aerodynamic camber effect

Y_{uv}^{vt} , lift slope effect

Y_{min}^{vt} , stall effect

7. Total Power Required

Total power due to the main rotor, tail rotor, wing, and miscellaneous effects are summed giving the total power output by the engine.

$$\text{Total power required} = P^{\text{mr}} + P^{\text{tr}} + P^{\text{fus}} + P^{\text{wng}} + P^{\text{climb}}$$

$$P^{\text{mr}} = P_{\text{induced}}^{\text{mr}} + P_{\text{profile}}^{\text{mr}} + P_{\text{accessories}}^{\text{mr}}$$

(Note: An estimate of power required for accessories can be found in Reference 12.)

$$P_{\text{induced}}^{\text{mr}} = T \cdot v_i$$

$$P_{\text{profile}}^{\text{mr}} = \rho/2 \frac{C_{D_0} b c R}{4} \Omega R \left[(\Omega R)^2 + 4.6 (U_a^2 + v_a^2) \right]$$

$$P^{\text{tr}} = P_{\text{induced}}^{\text{tr}} = T^{\text{tr}} \cdot v_i^{\text{tr}}$$

$$P^{\text{fus}} = \left| X_{\text{fus}} \cdot U_a \right| + \left| Y_{\text{fus}} \cdot V_a \right| + \left| Z_{\text{fus}} \cdot (W_a - v_i) \right|$$

$$P^{\text{wng}} = \left| X^{\text{wng}} \cdot U_a \right|$$

$$P^{\text{climb}} = m \cdot g \cdot h$$

8. Summation of Force and Moment Equations

The first order effects of all components are summed in three force equations and three moments equations. The force due to gravity rotated through theta and phi are also included here:

$$X = -m g \sin \theta + X^{\text{mr}} + X^{\text{fus}} + X^{\text{wng}}$$

$$Y = m g \sin \theta \cos \phi + Y^{\text{mr}} + Y^{\text{tr}} + Y^{\text{vt}}$$

$$Z = m g \cos \theta \cos \phi + Z^{\text{mr}} + Z^{\text{fus}} + Z^{\text{ht}} + Z^{\text{wng}}$$

$$L = L^{mr} + L^{fus} + L^{tr}$$

$$M = M^{mr} + M^{fus} + M^{ht}$$

$$N = N^{mr} + N^{tr} + N^{vt}$$

The equations of motion are expressed in terms of body axis accelerations so that they may be directly integrated to yield body velocities.

9. Integration and Axis Transformation

As discussed in Reference 13 the algorithm used for numerical integration of states should be carefully chosen to minimize digital effects.

The body accelerations are integrated using a second order Adams method in order to account partially for the one-frame hold between control (acceleration) input and the integrated velocity output:

$$v_{n+1} = v_n + DT(1.5 a_n - 0.5 a_{n-1})$$

These body velocities are then converted to earth relative velocities using a common Euler angle direction cosine transformation.

Finally, the earth velocities are integrated to obtain earth positions using a trapezoidal integration method in order to account partially for the zero-frame hold between velocity and the integrated position output:

$$x_{n+1} = x_n + DT(0.5 v_n + 0.5 v_{n-1})$$

10. Summary of Model Parameters

A summary of all the parameters included in this model are given below according to each model component. More detailed definitions are given in Appendix D.

1. Main rotor

FS.HUB	Fuselage station of hub
WL.HUB	Water line location of hub
IS	Forward tilt of rotor shaft w.r.t. fuselage
E.MR	Effective hinge offset
I.B	Blade flapping inertia
R.MR	Radius of main rotor
RPM.MR	RPM of main rotor
CDO	Blade profile drag coefficient
A.MR	Blade lift curve slope
B.MR	Number of blades
C.MR	Blade chord
TWST.MR	Blade twist
K1	Blade pitch-flap coupling proportion

2. Fuselage

FS.FUS	Fuselage station of fuselage center of pressure
WL.FUS	Waterline station of fuselage center of pressure
XUU.FUS	Aerodynamic quadratic model constant
YVV.FUS	" " " "
ZWW.FUS	" " " "

3. Tail rotor

FS.TR	Fuselage station of tail rotor
WL.TR	Waterline station of tail rotor
R.TR	Radius of tail rotor
RPM.TR	RPM of tail rotor
A.TR	Blade lift curve slope
SOL.TR	Tail rotor solidity
TWST.TR	Blade twist

4. Horizontal tail

FS.HT	Fuselage station of horizontal tail
WL.HT	Waterline station of horizontal tail
ZUU.HT	
ZUW.HT	
ZMAX.HT	Quadratic max lift coeff of horizontal tail

5. Wing

FS.WN	Fuselage station of wing
WL.WN	Waterline station of wing
ZUU.WN	
ZUW.WN	
ZMAX.WN	Quadratic max lift coeff of wing
B.WN	Span

6. Vertical tail

FS.VT	Fuselage station of vertical tail
WL.VT	Waterline station of vertical tail
YUU.VT	
YUV.VT	
YMAX.VT	Quadratic max lift coeff of vertical tail

III. Model Matching and Estimation Procedures

In order to demonstrate model matching and estimation procedures, a model of the Bell AH-1S Cobra is developed. The actual code for this example version along with a list of symbols and a table of associated input parameters are presented in Appendices A, B, and C. An example involving the matching of actual flight data is presented in Appendix D for the Augusta Model 109 helicopter.

The primary sources which are used in the Cobra example are the flight manual (Reference 14), a manufacturer's stability and control package (Reference 15), a volume of Jane's (Reference 16), and a flight dynamics data report (Reference 17). Other useful references include the USAF Stability and Control Datcom (Reference 18), the U. S. Army Engineering Design Handbook (Reference 19) and the previously cited Stepniewski and Keyes reference.

In this section the method is described for determining the the individual components of the AH-1S and its associated parameters. There are 44 total parameters needed for this model. 22 of these are simple geometrical variables which can be easily obtained from scale drawings, from aircraft manuals, or even estimated from a picture of the aircraft.

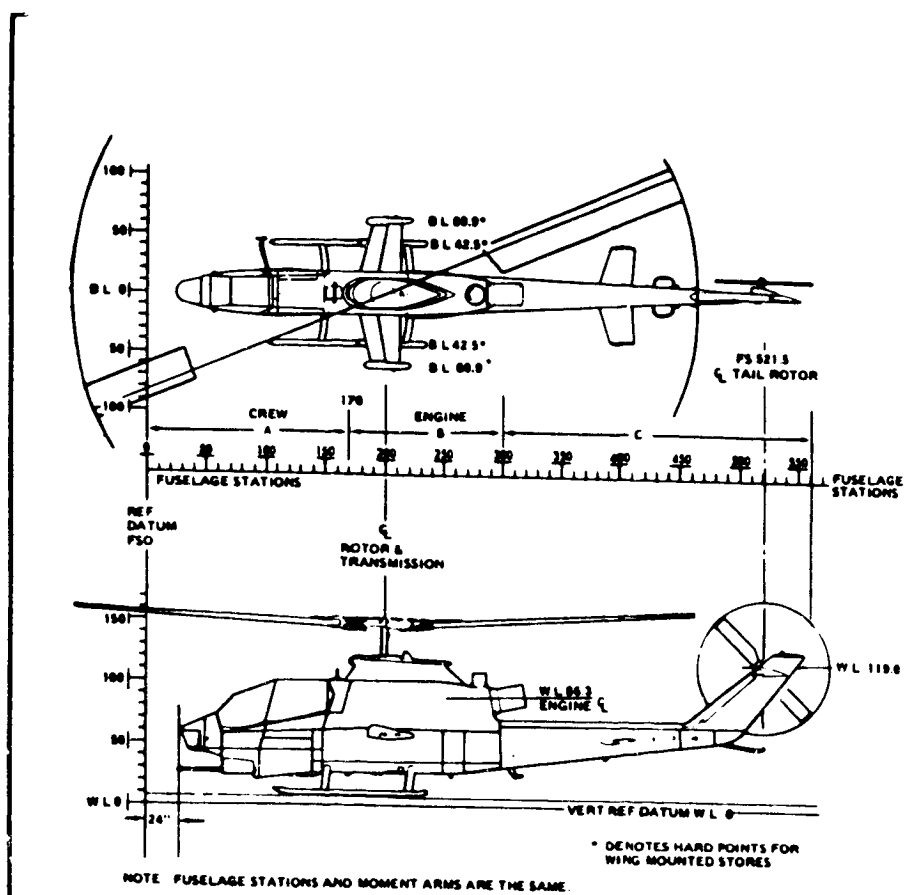
A. Mass, Loading, and Geometry Data

A substantial portion of the data required is either directly obtainable geometric data or common mass and loading data.

1. Geometric Data

Geometric parameters are easily obtained from aircraft drawings or reference literature. Figure 4, taken from the flight manual, provides a basis for geometric information. Note that positions of all major components are given relative to the manufacturer's reference system (fuselage stations, waterlines, and buttlines).

Explicit positions can be obtained for some features such as main rotor hub position and tail rotor hub. For airfoils it is generally sufficient to estimate and use the positions for one-quarter mean aerodynamic chord. The fuselage aerodynamic center is less clearly defined and must be estimated depending upon the shape. Appendages such as tail boom and landing gear can be considered in estimating the fuselage aerodynamic center.



209900-817A

Figure 6-1. Helicopter Station Diagram

6-2

COMPONENT	FS	WL
Main rotor hub	200	153
Tail rotor hub	521	119
Fuselage	200	65
Wing	200	65
Horizontal tail	400	65
Vertical tail	490	80

Figure 4. Basis for Geometric Data.

2. Mass and Loading Data

Values for normal operating gross weight and center of gravity are typically obtained from operating manuals. An example is shown in Figure 5. Specific choices will depend upon the general loading condition of interest. Here an intermediate loading is chosen which also corresponds to other available data.

Inertial data from the Reference 15 stability and control report are given in Table 4. While these do not correspond exactly to the loading chosen above, they can be easily rescaled by assuming a constant radius of gyration in each axis.

ORIGINAL PAGE IS
OF POOR QUALITY

TM 55 1520-236-10

EXAMPLE

WANTED

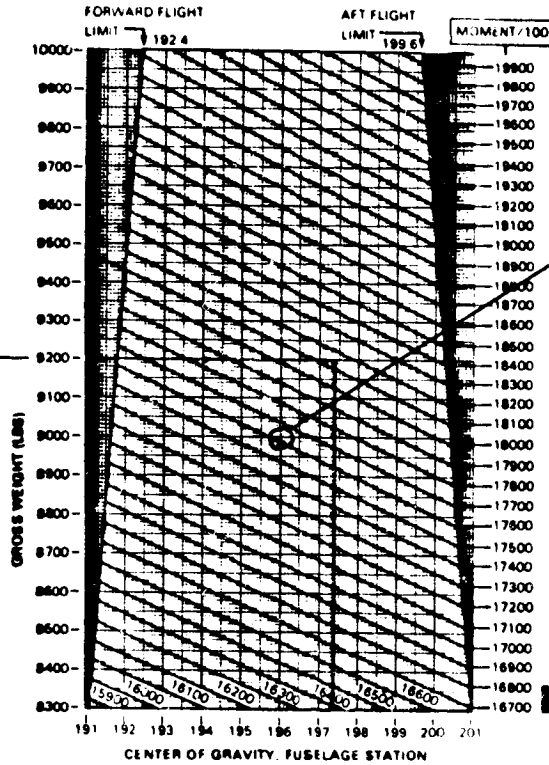
DETERMINE APPROXIMATE CENTER
OF GRAVITY
FOR KNOWN WEIGHT AND MOMENT

KNOWN

GROSS WEIGHT = 9200 POUNDS
MOMENT/100 = 18150 INCH-POUNDS

METHOD

MOVE RIGHT FROM 9200 POUNDS
TO APPROXIMATE MIDPOINT
BETWEEN 18100 AND 18200 IN-LB
DIAGONAL LINES
FROM THIS POINT MOVE DOWN
TO READ 187.4 ON CENTER OF
GRAVITY SCALE



Representative
weight and cg
chosen from
flight manual
operating envelope.
(9000 lb, FS 196)

201900-489 1G

Figure 6-9. Center of Gravity Limits Chart (Sheet 1 of 2)

6-17

Figure 5. Basis for Loading Data.

ORIGINAL PAGE IS
OF POOR QUALITY

Table 4. Basis for Inertial Data

62-099-012

4 BELL
HELICOPTER COMPANY

SUMMARY

TOTAL HELICOPTER MOMENTS OF INERTIA ABOUT HELICOPTER C.G.

<u>Condition</u>	<u>Weight (lbs.)</u>	<u>\bar{x} (in.)</u>	<u>\bar{z} (in.)</u>	<u>Moment of Inertia (Slug - Ft²)</u>			<u>Principal Axis (Nose Down Angle)</u>
				<u>Roll</u>	<u>Pitch</u>	<u>Yaw</u>	
(1) Weight Empty	5571.4	204	82	1990.4	10592.7	8878.2	
(2) Basic	8673.2	193	71	2843.0	13115.6	11264.0	6° 30'
(3) Hog	9501.1	194	68	4002.5	13082.3	11930.4	6° 37'
(4) Scout	9296.9	194	70	3195.3	13233.1	11606.7	6° 29'
(5) Most Forward	6606.2	191	78	2255.5	12462.4	10499.5	7° 19'
(6) Most Aft	7476.8	200	75	2265.6	11881.0	9903.8	4° 18'

Use as reference of data on this page is
subject to the restrictions on the title page.

A-11

B. Propulsion Data

Required propulsion data include power available for given operating conditions. These data can be found in Jane's under the appropriate propulsion system manufacturer as illustrated in Table 5. The specific information of interest here is the maximum continuous power rating for the AVCO Lycoming T53-L-703 gas turbine engine.

Other information needed consists of an approximate breakdown of power, including that due to accessories. Data from the Stepniewski and Keyes source are given in Table 6. These data will be used to estimate power losses from the computed power required by each of the components listed previously.

The basis for torque (power) available under various operating conditions is given in Figure 6. (Percent torque is assumed equal to percent power for the normal operating rpm=324 in this case.)

Table 5. Basis for Propulsion System Data.

AVCO LYCOMING GAS TURBINE ENGINES								
Manufacturer's and civil designation	Military designation	Type *	T-O Rating kN (lb st) or max kW (hp)	SFC μg/l; † mg/Ns (lb/hp; ‡lb/h/lb st)	Weight dry less tailpipe kg (lb)	Max dia mm (in)	Length overall mm (in)	Remarks
T5313B	—	ACFS	1,044 kW (1,400 shp)	98 (0-58)	245 (540)	584 (23)	1,209 (47-6)	Powers Bell 205A
T5317A	—	ACFS	1,119 kW (1,500 shp)	99-7 (0-59)	256 (564)	584 (23)	1,209 (47-6)	Based on T5319A
T5311A	—	ACFS	820 kW (1,100 shp)	115 (0-68)	225 (496)	584 (23)	1,209 (47-6)	Bell 204B
—	T53-L-13B	ACFS	1,044 kW (1,400 shp)	98 (0-58)	245 (540)	584 (23)	1,209 (47-6)	Advanced UH-1H, AH-1G
—	T53-L-703	ACFS	1,106 kW (1,485 shp)	101-4 (0-60)	247 (545)	584 (23)	1,209 (47-6)	Bell AH-1Q, AH-1STOW/Coon
LTC1K-4K	—	ACFS	1,157 kW (1,550 shp)	98-7 (0-584)	234 (515)	584 (23)	1,209 (47-6)	Bell XV-15
—	T53-L-701	ACFP	1,082 kW (1,451 ehp)	101-4 (0-60)	312 (688)	584 (23)	1,483 (58-4)	Grumman OV-1D
—	YT55-L-9	ACFP	1,887 kW (2,529 ehp)	102-7 (0-608)	363 (799)	615 (24-2)	1,580 (62-2)	Piper Enforcer
—	T55-L-7C	ACFS	2,125 kW (2,850 shp)	101-4 (0-60)	267 (590)	615 (24-2)	1,118 (44)	Boeing CH-47B, Bell 214A
T5508D (LTC4B-8D)	—	ACFS	2,186 kW (2,930 shp)	100-1 (0-592)	274 (605)	610 (24)	1,118 (44)	Bell 214A, 214B
—	—	—	flat-rated to 1,678 kW (2,250 shp)	106-0 (0-628)	—	—	—	—
—	T55-L-11A †	ACFS	2,796 kW (3,750 shp)	89-6 (0-53)	322 (710)	615 (24-2)	1,181 (46-5)	Boeing CH-47
LTC4B-12	—	ACFS	3,430 kW (4,600 shp)	86-2 (0-51)	329 (725)	615 (24-2)	1,118 (44)	Improved T55-L-11A
ALF 101	—	ACFF	7-2 kN (1,620 lb)	†10-19 (†0-36)	156 (343)	584 (23)	890 (35)	NASA QCGAT
ALF 502R-3	—	ACFF	29-8 kN (6,700 lb)	†11-64 (†0-411)	565 (1,245)	1,059 (41-7)	1,443 (56-8)	BAC 146
ALF 502L/L-2	—	ACFF	33-4 kN (7,500 lb)	†12-1 (†0-428)	590 (1,298)	1,059 (41-7)	1,487 (58-56)	Canadair CL-600 Challenger

*ACFS = axial plus centrifugal, free-turbine shaft; ACFP = axial plus centrifugal, free-turbine propeller; ACFF = axial plus centrifugal, free-turbine fan
 †Applies to T55-L-11A, C*, D, E* and 712*, those designated ** having 2% min contingency rating of 3,357 kW (4,500 shp).

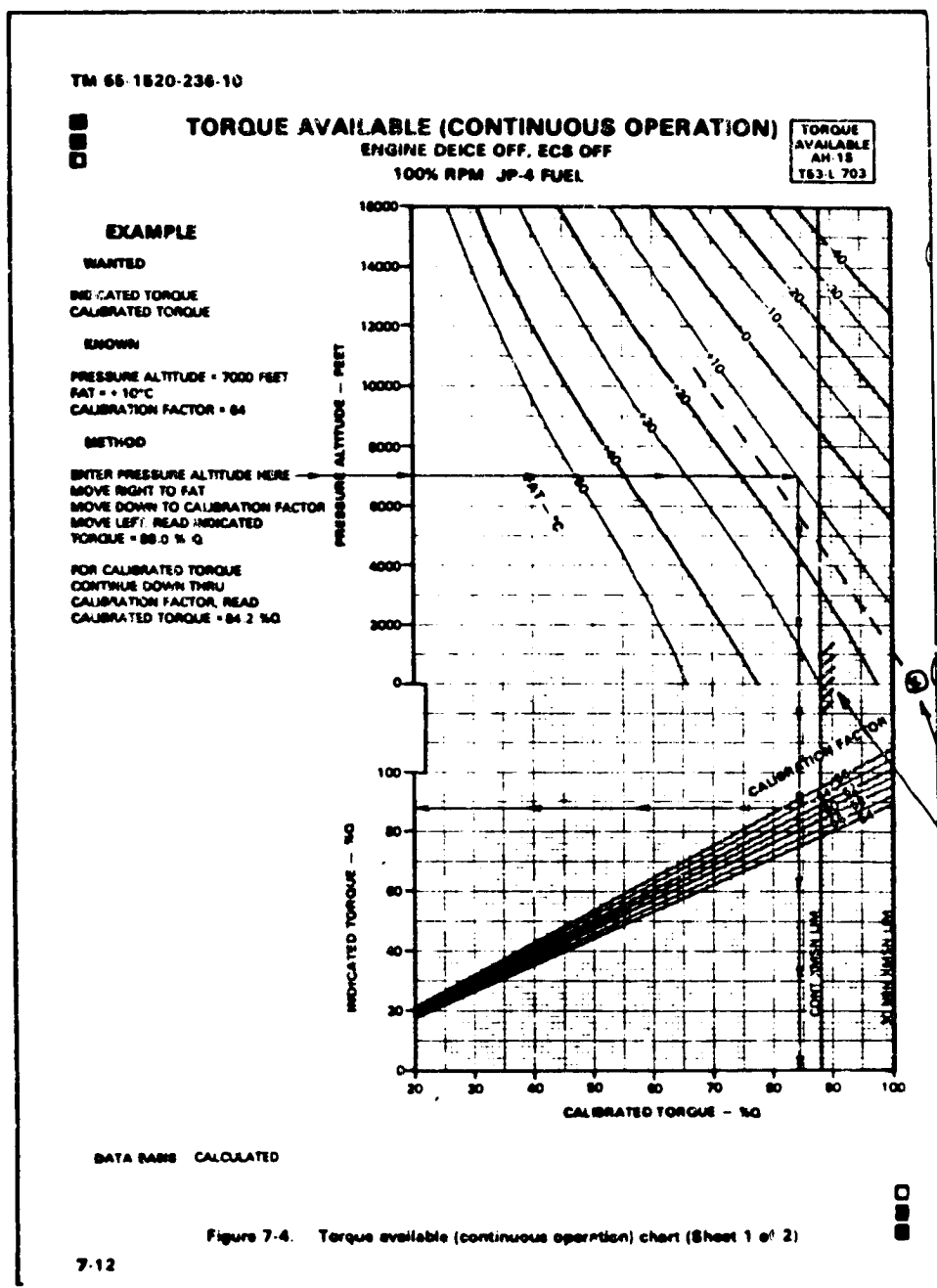
Table 6. Assumed Breakdown of Power Absorption.

	% Total Power in Hover	% Total Power Max Forward
Main rotor induced power	65	15
Main rotor profile power	15	50
Fuselage parasite power	5	25
Tail rotor total power	10	5
Misc. and accessories	5	5

(NOTE: Power losses due to wing stall should also be considered where the effect is suspected to be significant. It will be neglected in this example.)

ORIGINAL PAGE OF POOR QUALITY

ORIGINAL PAGE IS
OF POOR QUALITY



For sea level, std day;
torque is limited by
max continuous
operating condition.
(88%)

Figure 6. Basis for Torque (Power) Limits.

C. Rotor Data

Rotor system characteristics consist of geometric, aerodynamic, and operating condition features. Most of the geometric data including size and number of blades and hub center are easily found in flight manuals. Operating conditions, namely the normal operating rpm, are likewise obtained.

The main aerodynamic parameters include the effective section lift curve slope and profile drag coefficient. Commonly accepted values of 5.7 and .006, respectively, are sufficient starting points.

The most crucial rotor parameters, however, are those relating to the effective flapping stiffness or hinge offset. These data are generally found only in manufacturers design reports. Of course in the case of a simple teetering rotor the effective hinge offset is zero. Articulated rotor designs are also fairly easy to represent as long as the geometric hinge offset is known. The most difficult variety to model is the hingeless rotor since both an effective hinge offset and flapping spring must be determined.

Useful auxiliary information for modeling the rotor system is response data which provides direct indication of the unaugmented pitch and roll damping.

D. Aerodynamic Features

Aside from the rotor system aerodynamics, parameters must be estimated for the airfoil and fuselage components. The techniques for doing so are common and require little effort. If manufacturer's stability and control data are available these calculations are trivial. Otherwise, one can refer to estimation handbooks such as the USAF DATCOM (Reference 18).

Airfoil lift parameters involve three main features: camber and incidence, circulation lift, and stall. The first two are highly dependent upon geometry and the third on maximum lifting performance.

Relationships which are needed for setting parameters involve the quadratic aerodynamic parameters and the more common non-dimensional aerodynamic coefficients. These are given below for use in the estimation procedures described in Figure 7. The equations are for the horizontal tail, but the other airfoil surfaces are similar.

Estimates typical for airfoils:

$z_{uu}^{ht} = -S^{ht} C_{L_o}^{ht}$; C_{L_o} is set by both camber and incidence of the airfoil.

$z_{uw}^{ht} = -S^{ht} C_{L_\alpha}^{ht}$; note that $C_{L_\alpha} \approx \frac{2\pi R}{R+2}$

$z_{min}^{ht} = -S^{ht} C_{L_{max}}^{ht}$; typical values are 1.5 to 3 depending upon aspect ratio.

Similarly, fuselage drag estimates can be made for each of the three axes using available drag data.

Estimates typical for fuselage drag:

$$x_{uu}^{fus} = -S^{fus} C_D$$

where S^{fus} is the projected frontal area

and C_D can be estimated using numerous textbook tabulations of 3-dimensional drag. This will vary for each axis.

WING:

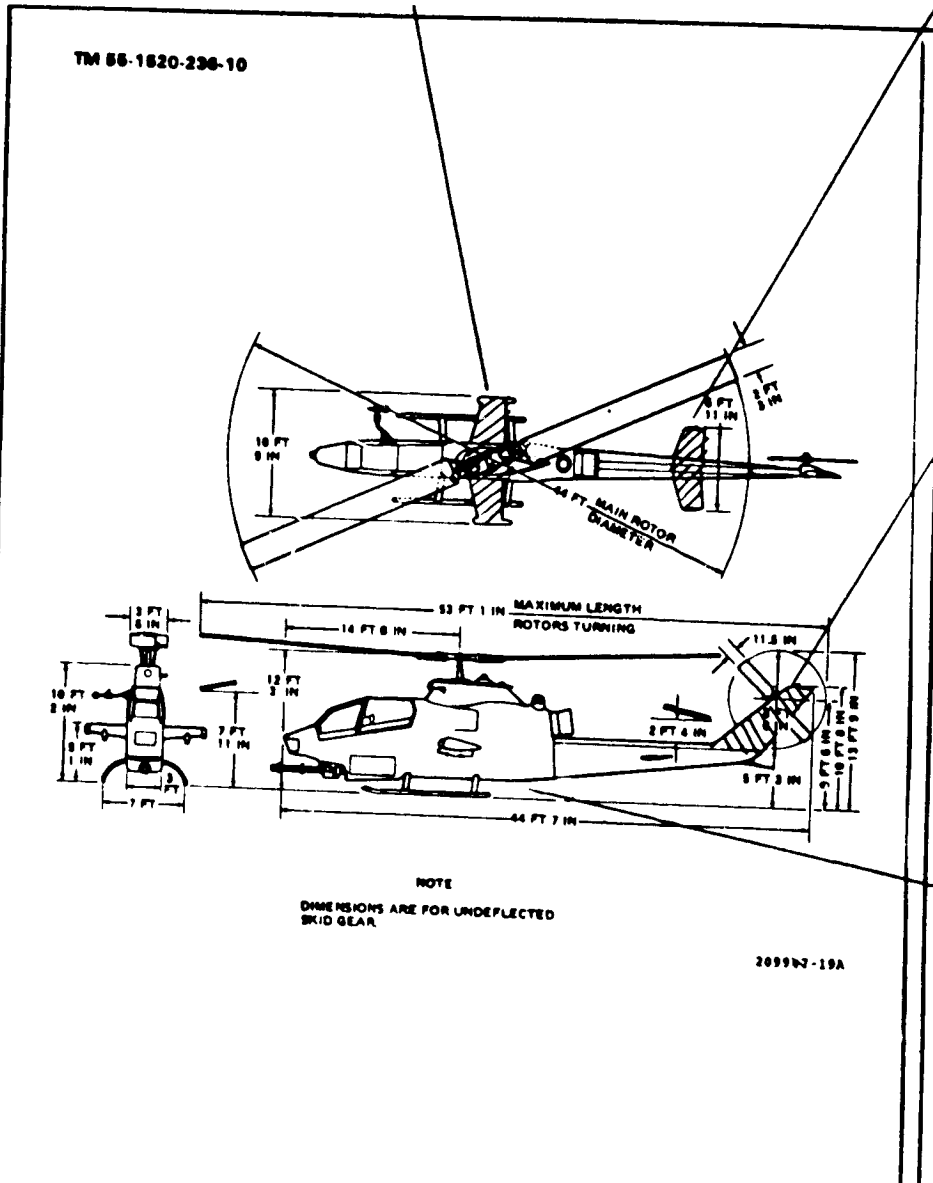
span = 10.75' (based on $i = 14^\circ$,
 chord = 3.0' $C_{L_0} \approx 1.2$,
 area = 32.25 ft² assume $C_{L_{max}} \approx 2$)
 aspect ratio = 3
 $C_{L_\alpha} \approx \frac{2\pi AR}{R+2} = 5$

HORIZONTAL TAIL:

span = 7'
 chord = 2.25'
 area = 16 ft²
 aspect ratio = 3
 $C_{L_\alpha} = 5$

VERTICAL TAIL:

span = 5'
 chord = 3.3'
 area = 17 ft²
 aspect ratio = 1.5
 $C_{L_\alpha} = 2.7$
 (assume $C_{L_{max}} \approx 3$)



NOTE
 DIMENSIONS ARE FOR UNDEFLECTED
 SKID GEAR

FUSELAGE:

assumed drag
 coefficients:
 front, 0.2
 side, 2.0
 plan, 0.7

Figure 2-2 Principal Dimensions (Typical)

2-4

Figure 7. Basis for Initial Estimates of Aerodynamic Parameters.

E. Hover Performance

The parameters listed above provide a starting point for the math model. Additional flight manual and available flight data will serve to make refinements in model response and performance characteristics.

The first adjustment of model parameters can be made based on the flight manual hover performance as shown in Figure 8. Here the percent maximum torque is given for a specific hover condition.

The factors which can be adjusted to achieve a good match are the power losses due to accessories, downwash on the fuselage and horizontal airfoils, or main rotor induced velocity factor (if included).

HOVER
 ALL CONFIGURATIONS 100% RPM
 LEVEL SURFACE CALM WIND

HOVER
 AM 15
 T63 L 703

EXAMPLE

WANTED

TORQUE REQUIRED TO HOVER

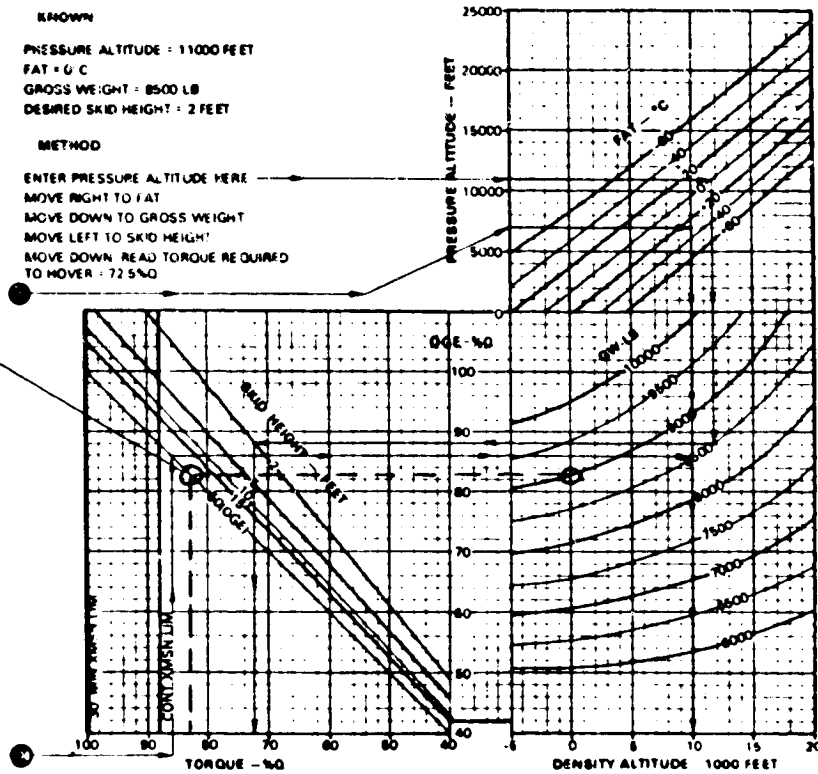
KNOWN

PRESSURE ALTITUDE : 11000 FEET
 FAT + G C
 GROSS WEIGHT : 8500 LB
 DESIRED SKID HEIGHT : 2 FEET

METHOD

ENTER PRESSURE ALTITUDE HERE
 MOVE RIGHT TO FAT
 MOVE DOWN TO GROSS WEIGHT
 MOVE LEFT TO SKID HEIGHT
 MOVE DOWN READ TORQUE REQUIRED
 TO HOVER : 72.5%

Torque req'd
 for OGE hover.
 (1232 hp)



DATA BASIS DERIVED FROM FLIGHT TEST

BS40 Figure 7-5 Hover chart (Sheet 2 of 2)

Figure 9. Basis for Hover Power Required.

ORIGINAL PAGE IS
 OF POOR QUALITY

F. Forward Flight Data

Up to this point model adjustments have centered on the main rotor system since body drag has been low due to the hover condition. With the consideration of forward flight the fuselage now plays a major role in limiting maximum speed and climb performance.

The main set of data useful for adjusting fuselage drag are given in Figure 9 from the flight manual. Note that the primary information is the torque required as a function of flight condition and loading. The two main features on this plot are the maximum speed at continuous operating torque and the torque and speed for level flight at minimum power.

Additional information is given in Figure 10 with the maximum rate of climb corresponding to an increase in torque.

Finally in Figure 11 data are given for the maximum glide and minimum rate of descent. These are useful for setting the effective full-down collective pitch stop.

TM 55-1520-236-10

CRUISE

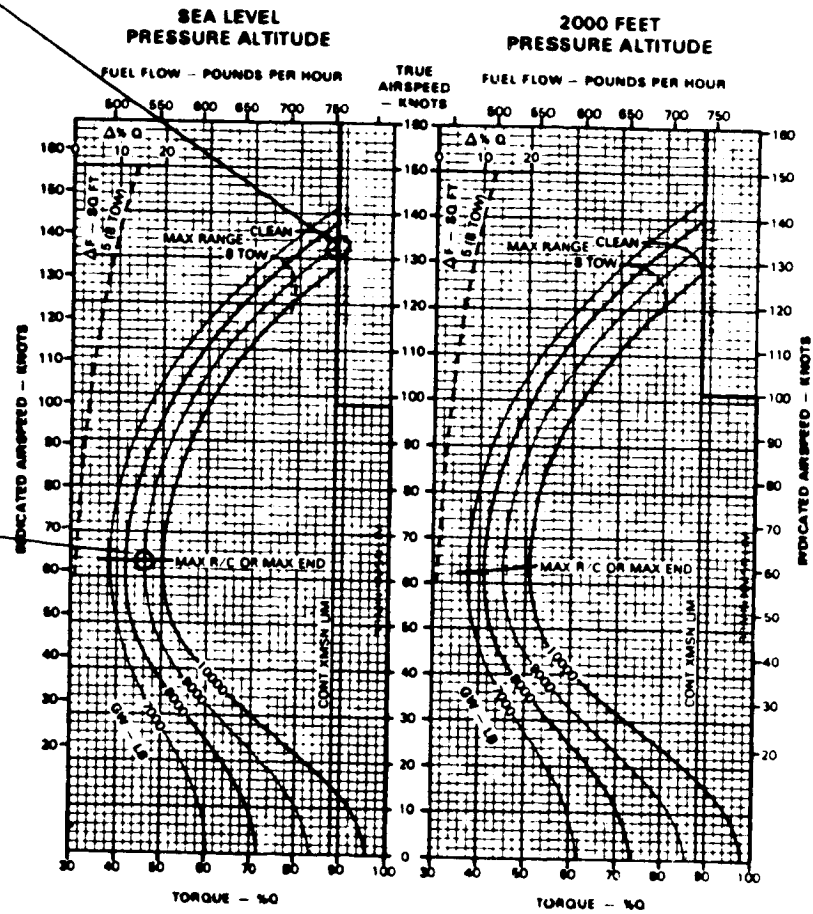
PRESSURE ALTITUDE - SEA LEVEL TO 2000 FEET
100% RPM, CLEAN CONFIGURATION, JP-4 FUEL

CRUISE
AM 15
T83 L 703

FAT = +15°C

Torque for max
level speed.
(133 kt @ 88%)

Torque and speed
for level flight at
min power.
(64 kt @ 46%)



BS40 Figure 7-7 Cruise Chart (Sheet 14 of 23)

7-34

Figure 10. Basis for Forward Flight Speeds and Power Required.

ORIGINAL PAGE IS
OF POOR QUALITY

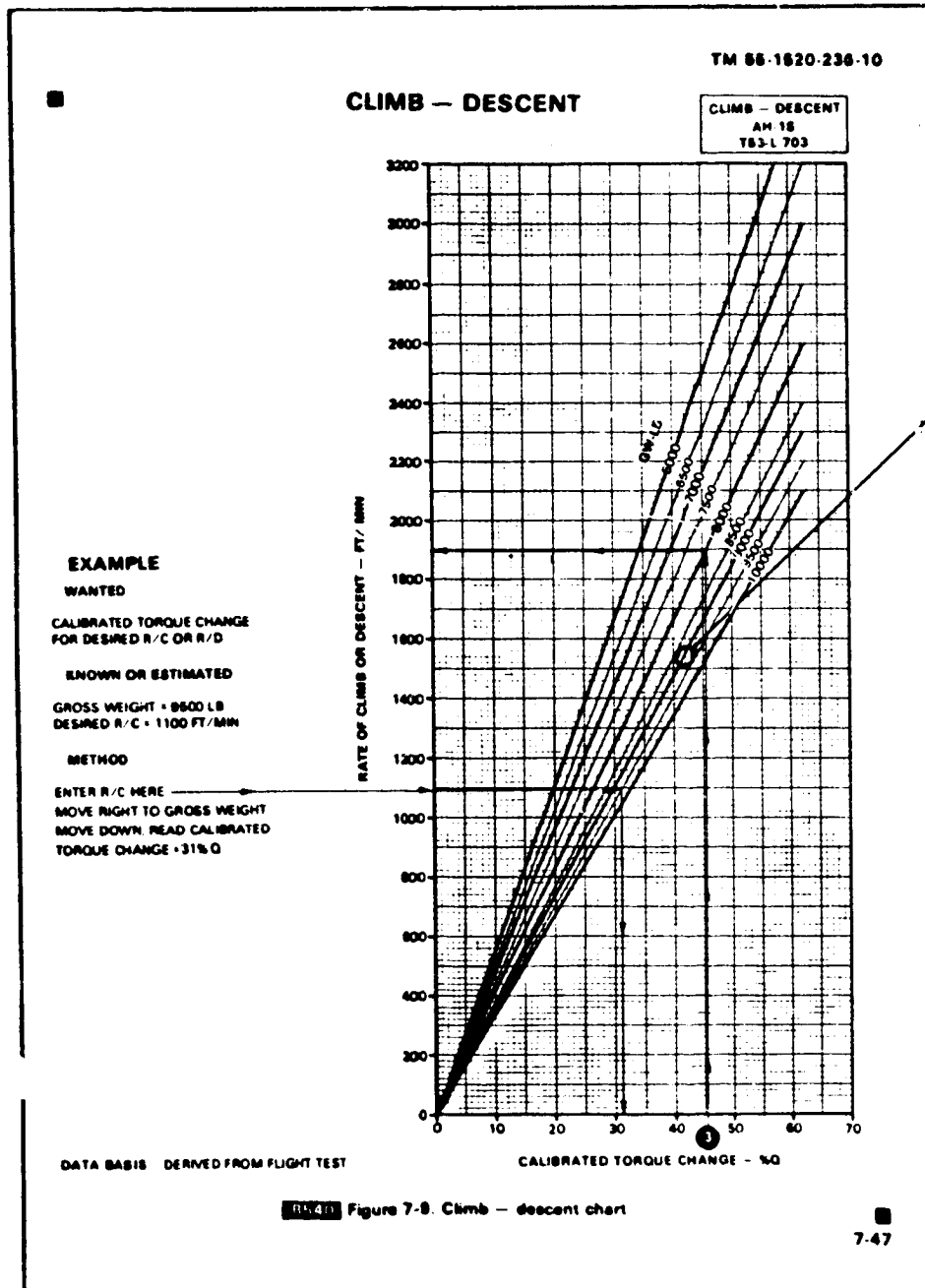


Figure 11. Basis for Max Rate of Climb Speed and Power Required.

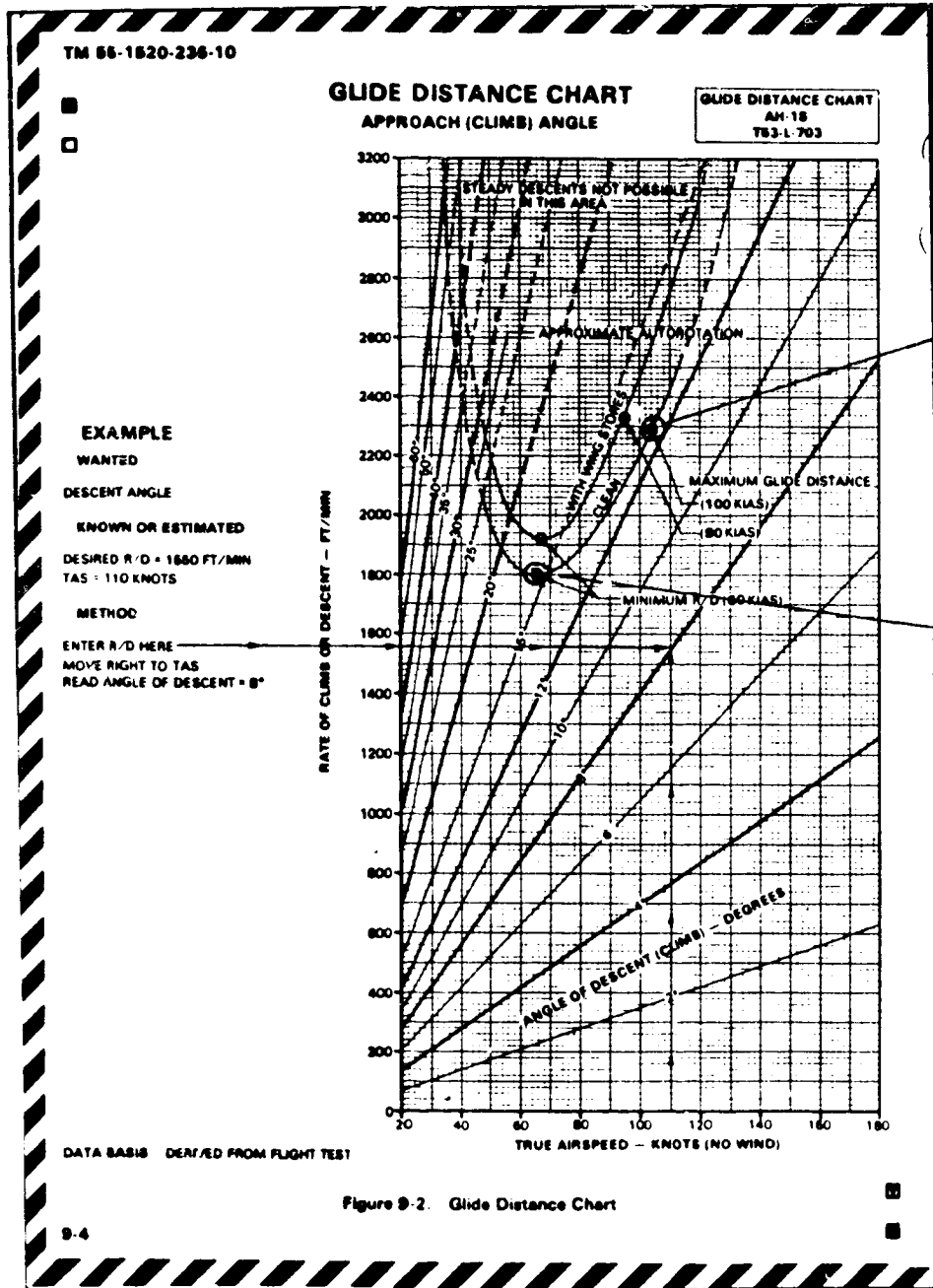


Figure 12. Basis for Max Glide Speed and Descent Angle.

ORIGINAL PAGE IS
OF POOR QUALITY

As a final note, the process of tuning model parameters should not be done without careful consideration of all secondary effects. The best policy is to avoid making anything other than simple direct first-principles corrections. There is substantial redundancy in some of the data shown here, and it is not possible to achieve perfect matches in all respects. One needs to exercise judgment in the degree of accuracy required as a function of the model application.

OFFICE OF THE
OF POOR QUALITY

IV. Checkout Procedures

A. General

As discussed earlier, model complexity can hamper the thoroughness of simulator computer program implementation and checking. However, the model presented here can be fully checked with reasonable effort. This is due to the small number of model constants and degrees of freedom, and minimal program branching. The recommended checking procedure involves the following elements:

- Use of an independent operating program.
- Verification of trim points.
- Verification of state transitions through n steps.
- Overlay of time histories.
- Identification of dominant response modes.

Some of these steps are redundant but nevertheless serve to build confidence in the correctness of the math model implementation at only minimal added cost. The following is a brief discussion of each element.

B. Discussion of Checkout Procedure Elements

1. Independent Operating Program

As a general rule, math model checkout should be accomplished using an independent implementation and check source. Furthermore, not only should an independent program be used but also an independent computer.

This math model form enables the user to develop a math model version on a small desktop microcomputer and run complete sets of check cases well in advance of using the simulator computer facilities.

The specific computer system used to develop and run this math model consisted of a Compaq 286 desktop computer with 640K working memory running Microsoft Basic. Only an interpreter mode was used although a Basic compiler is available. The interpreter permits a highly efficient interaction between the model developer and the computer system.

2. Trim Point Verification

A check of static trim points gives an initial indication of correct model implementation. The full operating envelope can be covered with just a few cases and possible discrepancies isolated to airspeed, vertical velocity, or controls. A cursory check of suspected parameters or component equations can usually lead to simple corrections. Trim solutions should be correct prior to proceeding to the next item.

A sample of the trim solution printout is given in Figure 12. This same format is displayed during the trimming process so that one can observe whether there are difficulties in iterating on a solution.

```
TRIM CALCULATIONS

HEFH2: FULL UTILITY VERSION
CONFIGURATION: 102 AH-1S
05-25-1987 16:09:55

Pdot = 1.05E+00 DC = 15.7
Qdot = -1.44E-01 a1 = 1.3
Rdot = 3.28E-03 b1 = -2.1
Udot = -4.88E-02 DTR = 1.02E+01
Vdot = -3.87E-02 Theta = -1.3
Wdot = 1.41E-03 Phi = -1.02E+00
aldot = -6.01E-02 B1 = -1.30E+00
bidot = 9.80E-02 A1 = -2.05E+00
Q = 1.34E+04 HP = 973
Vi = 35.8 Thrust = 9256
Vi.tr = 47.9 T.tr = 618
VB(1) = 0.00E+00 Xdot = 0.00E+00
VB(2) = 0.00E+00 Hdot = 0.0
VB(3) = 0.00E+00 Gamma = 0.00E+00

VT = 0.0
Hit (Q) to freeze trim anytime

Trimmed: Hit PRtSC to make hard copy
Hit RETURN to continue
```

Figure 13. Sample of Trim Point Printout.

3. State Transition Verification

Given that static solutions are valid, the dynamic response characteristics should be examined next. Correct operation is indicated by tracking several discrete state variable transitions and comparing with independently obtained check values. This is made feasible by restricting the number of degrees of freedom and levels of numerical integration. For example, only about six transitions for each control variable are needed to excite each term in the model equations.

In order to thoroughly check state transitions, a table overlay is recommended. This is accomplished by duplicating the state transition printout format of the checkout computer with that of the simulator computer. The original checks can be printed on transparencies then directly overlaid with the simulator printout.

7. Examples of the state transition checks are given in Table

ORIGINAL PAGE IS
OF POOR QUALITY

ORIGINAL PAGE IS
OF POOR QUALITY

Table 7. Sample of State Transition Checks.

05-26-1987

CONFIGURATION: 102
MELCORP/EE : AM-15
MESH : 9600
SI : .025
CONTROL DC(2) STEP INPUT = 1 DEGREES
NOTE: All angle units are degrees

TIME	DC(1)	DC(2)	DC(3)	DC(4)	VA(1)	VA(2)	VA(3)	VA(4)	VA(5)	VA(6)	VB(1)	VB(2)	VB(3)	VB(4)	VB(5)	VB(6)
0.0000	15.6852	-1.0532	-1.2974	10.1515	0.000	0.000	0.000	0.000	0.000	0.000	0.000	0.000	0.000	0.000	0.000	0.000
0.0250	15.6852	-1.0532	-1.2974	10.1515	0.000	0.000	0.000	0.000	0.000	0.000	-0.002	0.002	0.000	0.141	0.003	0.000
0.0500	15.6852	-1.0532	-1.2974	10.1515	-0.002	0.002	0.000	0.141	0.003	0.000	-0.006	0.008	0.000	0.455	0.016	0.000
0.0750	15.6852	-1.0532	-1.2974	10.1515	-0.006	0.008	0.000	0.455	0.016	0.000	-0.009	0.017	0.000	0.868	0.031	0.001
0.1000	15.6852	-1.0532	-1.2974	10.1515	-0.009	0.017	0.000	0.868	0.031	0.001	-0.013	0.028	0.000	1.341	0.046	0.002
0.1250	15.6852	-1.0532	-1.2974	10.1515	-0.013	0.028	0.000	1.341	0.046	0.002	-0.017	0.029	0.000	1.847	0.058	0.002
0.1500	15.6852	-1.0532	-1.2974	10.1515	-0.017	0.029	0.000	1.847	0.058	0.003	-0.020	0.052	0.000	2.364	0.067	0.005
0.1750	15.6852	-1.0532	-1.2974	10.1515	-0.020	0.052	0.000	2.364	0.067	0.005	-0.022	0.066	0.000	2.880	0.074	0.007

Table 7, Concluded.

IE (1)	IE (2)	VE (2)	VE (3)	VE (4)	VE (5)	VE (6)	AB (1)	AB (2)	AB (3)	AB (4)	AB (5)	AB (6)	IE (1)	IE (2)	IE (3)	IE (4)	IE (5)	IE (6)	bis	ais
0.000	0.000	0.000	0.000	0.000	0.000	0.000	-0.049	-0.029	0.001	1.055	-0.144	0.007	0.000	0.000	0.000	-1.020	-1.255	0.000	0.023	-0.036
0.002	0.000	0.141	0.002	0.000	0.000	0.000	-0.072	0.037	0.001	4.104	0.025	0.003	-0.000	0.000	0.000	-1.018	-1.255	0.000	0.024	-0.034
0.008	0.000	0.455	0.015	0.000	0.000	0.000	-0.117	0.179	0.001	9.756	0.351	0.008	-0.000	0.000	0.000	-1.011	-1.255	0.000	0.025	-0.029
0.017	0.000	0.868	0.021	0.000	0.000	0.000	-0.142	0.295	0.001	14.264	0.522	0.019	-0.000	0.000	0.000	-0.994	-1.254	0.000	0.026	-0.026
0.023	0.000	1.341	0.046	0.001	0.001	0.001	-0.147	0.382	0.001	17.363	0.566	0.032	-0.001	0.001	0.000	-0.967	-1.253	0.000	0.026	-0.024
0.039	0.000	1.946	0.058	0.002	0.002	0.002	-0.140	0.445	0.001	19.288	0.510	0.046	-0.001	0.002	0.000	-0.927	-1.252	0.000	0.025	-0.022
0.052	0.000	2.364	0.067	0.004	0.004	0.004	-0.128	0.491	0.001	20.232	0.415	0.061	-0.001	0.002	0.000	-0.874	-1.250	0.000	0.025	-0.021
0.066	0.000	2.850	0.074	0.005	0.005	0.005	-0.115	0.527	0.000	20.486	0.315	0.079	-0.002	0.004	0.000	-0.809	-1.248	0.000	0.025	-0.021

ORIGINAL PAGE IS
OF POOR QUALITY

4. Time History Overlays

In theory the combination of static and state transition checks should be sufficient to demonstrate agreement with the independent model implementation. However, additional confidence is gained by selecting several time history cases to overlay. These can be supplemented by checking dominant response modes based on transfer function solutions from the original independent check model.

Useful time histories to consider are angular rates for both on- and off-axes for a given control input. This checks both the dominant response modes and the amount of off-axis cross coupling. Examples are shown in Figure 13 corresponding to the previous check information.

STANDARDIZATION
OF PAPER QUALITY

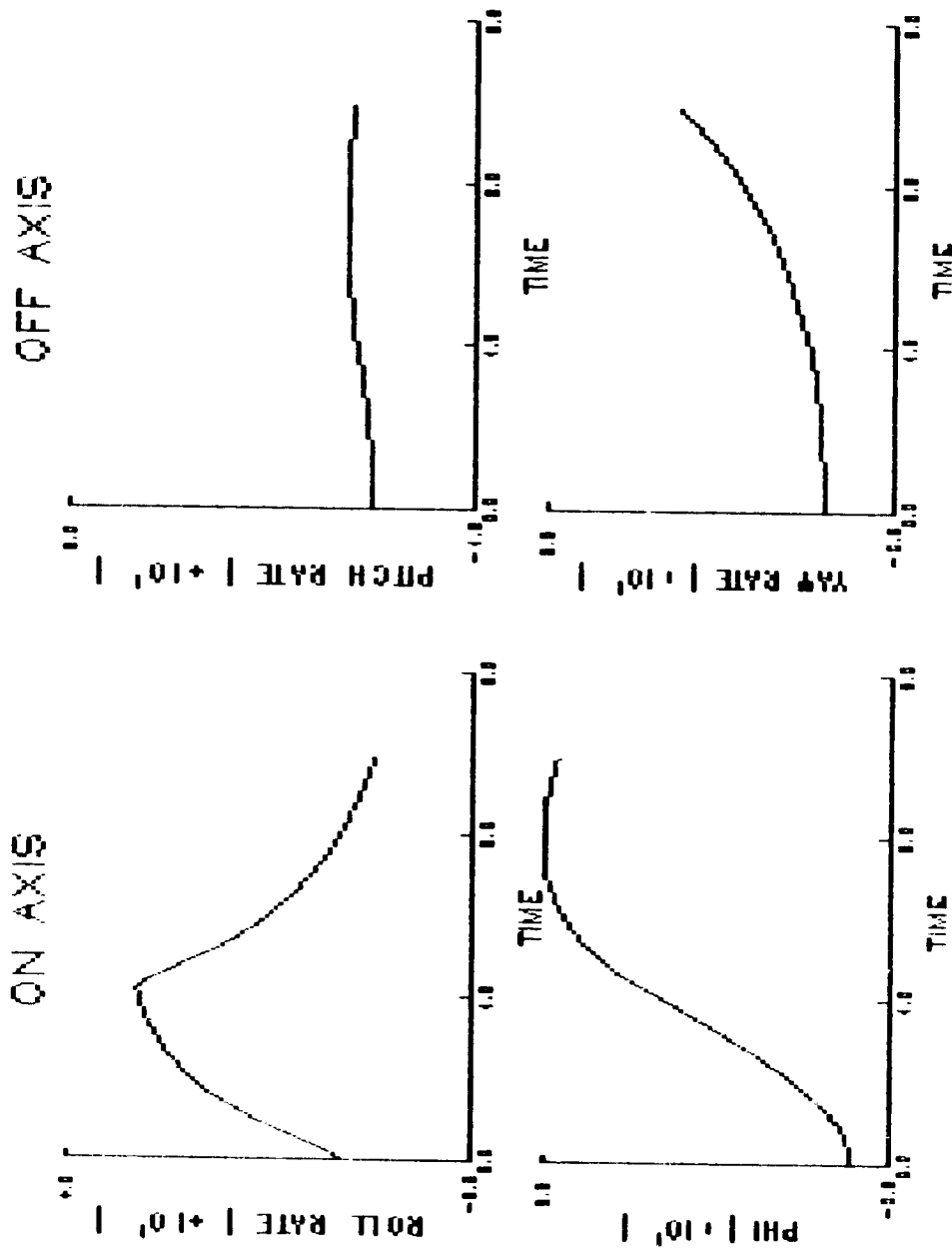


Figure 13. Examples of Time Histories to be Used for Overlays.

5. Dominant Response Identification

It is also useful to supplement the above checks with a comparison of identified dominant response features from the simulator computer with those features observed or computed from the independent checkout version. This is particularly important for handling qualities investigations.

Dominant modes are examined by exciting an axis with the corresponding direct control and scaling the appropriate first- or second-order response features from the respective motion traces. The on-axis traces presented earlier in Figure 13 serve this purpose for extracting short-term pitch response information.

V. Model Extensions and Refinements

The example which has been presented above can be modified in a number of ways in order to address specific simulation needs. The above math model can be either simplified or made more sophisticated. The following is a discussion of some possible extensions and refinements.

A. Flight Control System

There is no flight control system included in the above model other than conventional aerodynamic interfaces such as cyclic, collective, and tail rotor controls. Addition of a flight control system requires definition of relationships between the cockpit manipulator and the above aerodynamic controls plus any stability and control augmentation systems.

As with the basic airframe math model, definition of flight controls can be done with a wide range of computational complexity. However the same considerations can be applied in order to match the level of complexity with user utility. The main question is to what degree can the simulator pilot observe or be influenced by math model intricacies.

B. Engine Governor

This aspect of the helicopter math model can be important for tasks involving maneuvering or aggressive control of collective pitch.

The above math model is designed to accommodate an engine-governor system since rotor speed is explicit in the equations. It is necessary only to add appropriate engine governor equations of motion prior to computation of the main rotor thrust.

In general, only a second-order engine governor response is required in order to handle the effective spring-mass-damper action of the main rotor combined with the propulsion system and governor control laws. An adequate model is described in Reference 20.

C. Ground Effect

The modeling of ground effect can be important for tasks involving hover under marginal performance conditions. Again, the computational complexity of such models can vary widely.

It is recommended that, as a first cut, ground effect be modeled as an induced-velocity efficiency factor which primarily affects the thrust and power required to hover. This efficiency factor can be adequately modeled as an exponential function of altitude. The exponential scale height and magnitude is easily quantified from the flight manual hover performance shown earlier in Figure 8.

D. Dynamic Inflow

For certain vertical response applications it may be important to model the effective lag in thrust due to a collective pitch change. This is typically a first-order lag in the range of 10 to 15 rad/sec and varies with the sign of the collective pitch change.

This effect can be modeled by setting a first-order lag on the calculation of thrust and induced velocity. Reference 21 can be consulted for guidance in setting values. Other forces and moments can also be affected by dynamic inflow as described in Reference 22.

E. Higher-Order Flapping, Coning, and Lead-Lag Dynamics

Higher order rotor system dynamics may be of interest when examining flight control system schemes or certain vibrational effects. However the modes can easily be outside the computational ability of the simulator or highly distorted by the motion system. Thus is crucial for the modeler to analyze computational requirements relative to capabilities.

REFERENCES

- 1 Heffley, R. K., S. M. Bourne, H. C. Curtiss, Jr., W. S. Hindson, and R. A. Hess. Study of Helicopter Roll Control Effectiveness Criteria. NASA CR 117404 (USAAVSCOM TR 85-A-5). April 1986.
- 2 Heffley, R. K., S. M. Bourne, and M. A. Mnich. Helicopter Roll Control Effectiveness Criteria, Manudyne Report 83-2-2 (forthcoming NASA CR/AVSCOM TR), May 1987.
- 3 Talbot, Peter D., Bruce E. Tinling, William A. Decker, and Robert T. N. Chen. A Mathematical Model of a Single Main Rotor Helicopter for Piloted Simulation, NASA TM 84281, September 1982.
- 4 McFarland, R. E., CGI Delay Compensation, NASA TM-84281, January 1986.
- 5 Howlett, J. J., UH-60A Black Hawk Engineering Simulation Program: Volume I--Mathematical Model, NASA CR 166309, December 1981.
- 6 Chen, R. T. N., Effects of Primary Rotor Parameters on Flapping Dynamics, NASA TP-1431, January 1980.
- 7 Blake, B. B. and I. B. Alansky, Stability and Control of the YUH-61A, AHS Annual National Forum, 1975.
- 8 Glauert, M. A., A General Theory of the Autogyro, Royal Aeronautical Establishment R. and M. No. 1111, November 1926.
- 9 Lock, C. N. H., Further Development of Autogyro Theory, Royal Aeronautical Establishment R. and M. No. 1127, March, 1927.
- 10 Lamb, Horace, "Hydrodynamics," Dover, New York, 1945.
- 11 Monk, Max M., The Aerodynamic Forces on Airship Hulls, National Advisory Committee for Aeronautics Report No. 184, 1923.
- 12 Stepniewski, W. Z. and C. N. Keys, "Rotary-Wing Aerodynamics," Dover, New York, 1984.
- 13 Heffley, R. K., Wayne F. Jewell, Richard F. Whitbeck, and Ted M. Schulman, The Analysis of Delays in Simulator Digital Computing Systems, Volume I, NASA CR-152340, February 1980.

- 14 Anon., Operator's Manual Army Model AH-1S (PROD) AH-1S (ECAS) AH-1S (Modernized Cobra) Helicopters, Departement of the Army, TM 55-1520-236-10, 11 January 1980.
- 15 Davis, John M., Stability and Control Data Summaries for the AH-1G and UH-1H Helicopters, Bell Helicopter Report 699-099-012, 9 January 1976.
- 16 Taylor, John W. R. ed., Jane's All the World's Aircraft 1980-81. Jane's Publishing Company Limited, London, 1980.
- 17 Heffley, Robert K., Wayne F. Jewell, John M. Lehman, and Richard A. Van Winkle, A Compilation and Analysis of Helicopter Handling Qualities Data, NASA CR 3144, August 1979.
- 18 Anon., USAF Stability and Control DATCOM, October 1960, revised April 1978.
- 19 Anon., U. S. Army Engineering Design Handbook, Part I, AMCP 706-201, August 1974, and Part II, AMCP 706-202, January 1976.
- 20 Corliss, Lloyd and Chris Blanken, A Simulation Investigation of the Effects of Engine and Thrust Response Characteristics on Helicopter Handling Qualities, NASA TM 85849, October 1983.
- 21 Chen, R. T. N. and William S. Hindson, Influence of Dynamic Inflow on Helicopter Vertical Response, NASA TM 88327, June 1986.
- 22 Gaonkar, G. H. and D. A. Peters, "Effectiveness of Current Dynamic-Inflow Models in Hover and Forward Flight." Journal of the American Helicopter Society, Volume 31-Number 2, April 1986, pp 47-57.

ORIGINAL PAGE IS
OF POOR QUALITY

APPENDIX A

BASIC PROGRAM LISTING OF MATH MODEL

```
1480 *****
1490
1500 Preliminary Calculations
1510
1520 *****
1530
1540 VT.IN.FPS = ABS(XDOT/COS(GAMMA.RAD))
1550 VT = VT.IN.FPS/FPS.PER.KNOT
1560 VT.IN.FPS.SQUARED = VT.IN.FPS ^ 2
1570 M = WT/GRAV
1580 OMEGA.MR = RPM.MR*2*PI/60
1590 OMEGA.TR = RPM.TR*2*PI/60
1600 V.TIP=R.MR*OMEGA.MR
1610 FR.MR = CDD*R.MR*B.MR*C.MR
1620 FR.TR = CDD*R.TR*B.TR*C.TR
1630 MF.LOSS = 90
1640 VTRANS = 50 : ' speed for transition from dihedral wake function
1650 TEMP.RATIO=1 - LAPSE.RT*H
1660 PRESS.RATIO = TEMP.RATIO^TEMP.EXP
1670 DENS.RATIO = PRESS.RATIO/TEMP.RATIO
1680 R0 = DENS.RATIO*RHO.SEA.LEVEL : R2=R0/2
1690 GAM.O.M.16 = R0*A.MR*C.MR*R.MR^4/I.B *OMEGA.MR/16*(1+B/3*E.MR/R.MR)
1700 KC = ( .75*OMEGA.MR*E.MR/R.MR / GAM.O.M.16 ) + K1 : ' flapping aero cpl
1710 ITB2.O.M = OMEGA.MR/(1+(OMEGA.MR/GAM.O.M.16)^2) : ' flapping x-cpl coef
1720 ITB = ITB2.O.M*OMEGA.MR/GAM.O.M.16 : ' flapping primary resp
1730 DL.D91 = B.MR/2*(1.5*I.B*E.MR/R.MR*OMEGA.MR*OMEGA.MR) : ' primary flapping stiffness
1740 DL.DA1=R2*A.MR*B.MR*C.MR*R.MR*V.TIP*V.TIP*E.MR/6 : ' cross flapping stiffness
1750 CT=WT/(R0*PI*R.MR*R.MR*V.TIP*V.TIP) : ' thrust coefficient
1760 A.SIGMA=4.MR*B.MR*C.MR/R.MR/PI : ' a x sigma
1770 DB1DV=2/OMEGA.MR/R.MR*(B*CT/A.SIGMA+(SQR(CT/2))) : ' TPP dihedral effect
1780 DA1DV=-DB1DV : ' TPP pitchup with speed
1790
1800 H.HUB = (WL.HUB-WL.CG)/12 : D.HUB = (FS.HUB-FS.CG)/12 : ' hub re cg
1810 H.FUS = (WL.FUS-WL.CG)/12 : D.FUS = (FS.FUS-FS.CG)/12 : ' fuselage re cg
1820 H.WN = (WL.WN -WL.CG)/12 : D.WN = (FS.WN -FS.CG)/12 : ' wing re cg
1830 H.HT = (WL.HT -WL.CG)/12 : D.HT = (FS.HT -FS.CG)/12 : ' horizontal tail re cg
1840 H.VT = (WL.VT -WL.CG)/12 : D.VT = (FS.VT -FS.CG)/12 : ' vertical fin re cg
1850 H.TR = (WL.TR -WL.CG)/12 : D.TR = (FS.TR -FS.CG)/12 : ' tail rotor re cg
1860
1870 RETURN
```

```

7500 *****
7510
7520 DYNAMICS: Dynamics subroutine
7530
7540 *****
7550
7560 ***** Preliminary calculations *****
7570
7580 C4 = COS(XE(4)) : S4 = SIN(XE(4)) : evaluate Euler angle trig fns
7590 C5 = COS(XE(5)) : S5 = SIN(XE(5))
7600
7610 VA(1)=VB(1) : -(VG(1)*C5) : evaluate relative air mass velocities
7620 VA(2)=VB(2) : -(VG(2)*C6-VG(1)*S6)
7630 VA(3)=VB(3) : -(VG(3)*C5+VG(1)*S5)
7640 VA(4)=VB(4) : -VG(4)
7650 VA(5)=VB(5)
7660 VA(6)=VB(6)
7670
7680 WTA=SQRT(VA(1)*VA(1)+VA(2)*VA(2)+VA(3)*VA(3))
7690
7700 ***** Rotor tip path plane dynamics *****
7710
7720 A.SUM= BV(8)-DC(2)+KC*BV(7)+DB1DV*VA(2) : b1 - A1 + e.a1 + db1/dv .V
7730 B.SUM= BV(7)+DC(3)-KC*BV(8)+DA1DU*VA(1) : a1 + B1 - e.b1 + da1/du .U
7740
7750 GR(7)= - ITB*B.SUM - ITB2.OM*A.SUM - VA(5) : a1.dot
7760 GR(8)= - ITB*A.SUM + ITB2.OM*B.SUM - VA(4) : b1.dot
7770
7780 BV(7)=BV(7) + ST*(A2*GR(7) + B2*AP(7)) : a1 updated
7790 BV(8)=BV(8) + ST*(A2*GR(8) + B2*AP(8)) : b1 updated
7800
7810 AP(7)=GR(7) : AP(8)=GR(8) : save past values
7820
7830 ***** Main Rotor thrust and induced velocity *****
7840
7850 WR = VA(3) + (BV(7) - IS)*VA(1) - BV(8)*VA(2) : z-axis vel re rotor plane
7860 WB = WR -2/3*OM*GA.MR*R.MR*(DC(1) + .75*TWST.MR): z-axis vel re blade
7870
7880 FOR I=1 TO 5 : iterative solution of thrust and induced vel
7890 THRUST.MR=(WB-VI.MR)*OMEGA.MR*R.MR*RHO*A.MR*B.MR*C.MR/R.MR/4
7900 VHAT.2=VA(1)^2 + VA(2)^2 + WR*(WR-2*VI.MR)
7910 VI.MR.2=SQRT((VHAT.2/2)*(VHAT.2/2)+(THRUST.MR/2/(RHO*PI*R.MR^2))^2) - VHAT.2/2
7920 VI.MR=SQRT(ABS(VI.MR.2)) : main rotor induced velocity
7930 NEXT I
7940
7950 ***** Fuselage *****
7960
7970 WA.FUS = VA(3) - VI.MR : include rotor downwash on fuselage
7980 D.FW=(VA(1)/(-WA.FUS)+(H.HUB-H.FUS))- (D.FUS-D.HUB) : pos of downwash on fus
7990
8000 X.FUS = R2 + XU.U.FUS * ABS(VA(1)) * VA(1) : drag force
8010 Y.FUS = R2 + YVV.FUS * ABS(VA(2)) * VA(2) : side-force
8020 Z.FUS = R2 + ZWW.FUS * ABS(WA.FUS) * WA.FUS : heave force
8030 L.FUS = Y.FUS*H.FUS

```

ORIGINAL PAGE IS
OF POOR QUALITY

ORIGINAL PAGE IS
OF POOR QUALITY

```

4167 M.FUS = Z.FUS*D.FW - X.FUS*H.FUS
4170
4181 P.INDUCED.MR = THRUST.MR * VI.MR
4189 P.CLIMB = WT*HDDT
4196 P.PARASITE = - X.FUS*VA(1) - Y.FUS*VA(2) - Z.FUS*WA.FUS
4203 P.PROFILE.MR = R2*(FR.MR/4)*OMEGA.MR*R.MR*(OMEGA.MR^2*R.MR^2 +
4210 4.B*(VA(1)*VA(1)+VA(2)*VA(2)))
4217 POWER.MR = P.INDUCED.MR + P.CLIMB + P.PARASITE + P.PROFILE.MR
4224 POWER.ROTOR.MR = P.INDUCED.MR + P.PROFILE.MR
4231 POWER.FUS = P.PARASITE
4238 TORQUE.MR = POWER.MR/OMEGA.MR
4245
4252 Compute main rotor force and moment components.
4259
4266 Y.MR = -THRUST.MR * (GV(7)-IS)
4273 Y.MR = THRUST.MR * GV(8)
4280 Z.MR = -THRUST.MR
4287 L.MR = Y.MR*H.HUB + DL.DB1*GV(8) + DL.DA1*(GV(7)+DC(3) - K1*GV(8))
4294 M.MR = Z.MR*D.HUB - X.MR*H.HUB + DL.DB1*GV(7) +DL.DA1*(-GV(8)+DC(2) - K1*GV(7))
4301 N.MR = TORQUE.MR
4308
4315 ***** Tail Rotor thrust and induced velocity *****
4322
4329 VR.TR = -(VA(2) - VA(6)*D.TR + VA(4)*H.TR) : ' velocity relative to rotor plane
4336 VB.TR = VR.TR +2/3*OMEGA.TR*R.TR*(DC(4)+TWST.TR*.75) : ' velocity relative to blade
4343
4350 FOR I=1 TO 5 : ' iterate on thrust and induced velocity
4357 THRUST.TR=(VB.TR-VI.TR)*OMEGA.TR*R.TR*RHO*A.TR*SOL.TR*PI*R.TR*R.TR/4
4364 VHAT.2=(VA(3)+VA(5)*D.TR)^2 + VA(1)^2 + VR.TR*(VR.TR-2*VI.TR)
4371 VI.TR.2=SQR((VHAT.2/2)*(VHAT.2/2)+(THRUST.TR/2/(RHO*PI*R.TR^2))^2) - VHAT.2/2
4378 VI.TR=SQR(ABS(VI.TR.2))
4385 NEXT I
4392
4400 POWER.TR = THRUST.TR*VI.TR
4407 Y.TR = THRUST.TR
4414 L.TR = Y.TR*H.TR
4421 N.TR = -Y.TR*D.TR
4428
4435 ***** Horizontal tail *****
4442
4449 D.DW=( VA(1)/(VI.MR-VA*3)*(H.HUB-H.HT) )-( D.HT-D.HUB-R.MR ) : ' dnwsh impinges on tail?
4456 EPS.HT=.5*(1+SGN(D.DW)) : ' uniform downwash field
4463 IF D.DW>0 AND D.DW<R.MR THEN EPS.HT= 2*(1-D.DW/R.MR) ELSE EPS.HT=0 : ' trianglr dnwsh
4470
4477 WA.HT = VA(3) - EPS.HT*VI.MR + D.HT*VA(5) : ' local z-vel at h.t.
4484 VTA.HT=SQR(VA(1)*VA(1)+VA(2)*VA(2)+WA.HT*WA.HT)
4491 Z.HT=R2*(ZUU.HT*ABS(VA(1))*VA(1) + ZUU.HT*ABS(VA(1))*WA.HT) : ' circulation lift on h.t.
4498
4505 IF ABS(WA.HT) .3*ABS(VA(1)) THEN Z.HT=R2*ZMAX.HT*ABS(VTA.HT)*WA.HT : ' surface stalled?
4512
4519 M.HT = Z.HT*D.HT : ' pitching moment
4526
4533 ***** Wing *****
4540

```

```

4000 WA.WN = VA(3) - VI.MR : ' local z-vel at wing
4010 VTA.WN = SQRT(VA(1)*VA(1) + WA.WN*WA.WN)
4020
4030 Z.WN=R2*(ZUU.WN*VA(1)*VA(1) + ZUW.WN*VA(1)*WA.WN) : ' normal force
4040 X.WN= -R2/F1/VTA.WN/VTA.WN*(ZUU.WN*VA(1)*VA(1)+ZUW.WN*VA(1)*WA.WN)^2 : ' induced drag
4050
4060 IF ABS(WA.WN)>.3*ABS(VA(1)) THEN Z.WN=R2*ZMAX.WN*ABS(VTA.WN)*WA.WN : ' surface stalled?
4070
4080 POWER.WN = ABS(X.WN*VA(1))
4090 POWER = POWER.MR + POWER.TR + POWER.WN + HP.LOSS*550
4100

```

***** Vertical tail *****

Compute aerodynamic forces on vertical tail

```

4110
4120
4130 VA.VT=VA(2)+VI.TR-D.VT*VA(6)
4140 VTA.VT=SQRT(VA(1)*VA(1)+VA.VT*VA.VT)
4150 Y.VT=R2*(YUU.VT*ABS(VA(1))*VA(1) + YUV.VT*ABS(VA(1))*VA.VT)
4160
4170 IF ABS(VA.VT)>.3*ABS(VA(1)) THEN Y.VT=R2*YMAX.VT*ABS(VTA.VT)*VA.VT : ' surface stalled?
4180
4190 L.VT = Y.VT*H.VT
4200 N.VT = -Y.VT*D.VT
4210

```

***** General force equations *****

```

4240 X.GRAV = -M*GRAV*S5 : gravity forces
4250 Y.GRAV = M*GRAV*S4*C5
4260 Z.GRAV = M*GRAV*C5*C4
4270

```

	gravity	M.R.	FUS.	T.R.	H.T.	WING	V.T.	component
4280								
4290								
4300	F(1) =	X.GRAV + X.MR	+ X.FUS			+ X.WN		: X-force
4310	F(2) =	Y.GRAV + Y.MR	+ Y.FUS + Y.TR				+ Y.VT	: Y-force
4320	F(3) =	Z.GRAV + Z.MR	+ Z.FUS +		+ Z.HT + Z.WN			: Z-force
4330	F(4) =		+ L.MR + L.FUS + L.TR				+ L.VT	: L-moment
4340	F(5) =		+ M.MR + M.FUS		+ M.HT			: M-moment
4350	F(6) =		+ N.MR		+ N.TR		+ N.VT	: N-moment
4360								
4370	F(7) =		GR(7)/ITB					: pitch flap
4380	F(8) =		SR(8)/ITB					: roll flap
4390								

IF CHECK=0 THEN GOSUB 7790 : fill force component array

Body Accelerations

```

4400 AB(1) = - (VB(5)*VB(3)-VB(6)*VB(2)) + F(1)/M
4410 AB(2) = (VB(4)*VB(3)-VB(1)*VB(6)) + F(2)/M
4420 AB(3) = (VB(1)*VB(5)-VB(4)*VB(2)) + F(3)/M
4430 AB(4) = F(4)/IX
4440 AB(5) = F(5)/IY - VB(4)*VB(6)*(IX-IZ)/IY + (VB(6)*VB(6)-VB(4)*VB(4))*IXZ/IY

```

ORIGINAL PAGE IS OF POOR QUALITY

ORIGINAL PAGE IS
OF POOR QUALITY

```
5140      AB(6) = F(6)/I2 + IX2*AB(4)/I2
5150
5160      Integrate Body Accelerations
5170
5180      FOR IX = 1 TO 6
5190      VB(IX) = VB(IX) + ST * (A1 * AB(IX) + B1 * AP(IX))
5200      AP(IX) = AB(IX) : REM SAVE ACCEL PAST VALUES
5210      NEXT IX
5220
5230      Transform to earth (A/C rel to deck) velocities
5240
5250      VE(1) = (VB(1) * C5 + VB(3) * S5) * C4 * COS(XE(6))
5260      VE(2) = VB(2)*COS(XE(6))+VB(1) * SIN(XE(6))
5270      VE(3) = (VB(1) * S5 - VB(3) * C5) * C4
5280      VE(4) = VB(4) + (VB(5) * S4 + VB(6) * C4) * TAN(XE(5))
5290      VE(5) = VB(5) * C4 - VB(6) * S4
5300      VE(6) = (VB(6) * C4 + VB(5) * S4) / C5
5310
5320      Integrate earth (A/C relative to deck) velocities
5330
5340      FOR IX = 1 TO 6
5350      VE(IX) = VE(IX) + ST * (A2 * VE(IX) + B2 * VP(IX))
5360      VP(IX) = VE(IX) : REM SAVE VEL PAST VALUES
5370      NEXT IX
5380
5390      TIME=TIME+ST
5400
5410      IF CHECK=1 THEN IF CHECK.LOOP<CHECK.LOOP.MAX THEN GOTO 3520
5420      IF CHECK=1 THEN GOSUB 8890
5430
5440      RETURN
```

APPENDIX B
DEFINITION OF PROGRAM SYMBOLS

A1	Numerical integration constant (Adams-two = 1.5).
A2	Numerical integration constant (trapezoidal = 0.5).
AB(i)	Body-axis acceleration vector.
AB(1)	Body x-axis acceleration (\dot{U}) component (ft/sec ²).
AB(2)	Body y-axis acceleration (\dot{V}) component (ft/sec ²).
AB(3)	Body z-axis acceleration (\dot{W}) component (ft/sec ²).
AB(4)	Body roll axis acceleration (\dot{P}) component (ft/sec ²).
AB(5)	Body pitch axis acceleration (\dot{Q}) component (ft/sec ²).
AB(6)	Body yaw axis acceleration (\dot{R}) component (ft/sec ²).
AB(7)	Lateral tip-path-plane angular rate (b_1) (rad).
AB(8)	Longitudinal tip-path-plane angular rate (a_1) (rad).
AP(i)	Past value of AB(i).
A.SIGMA	Product of lift-curve-slope and solidity.
B1	Numerical integration constant, 1-A1.
B2	Numerical integration constant, 1-A2.
C4	Cos[XE(4)] or Cos of roll Euler angle.
C5	Cos[XE(5)] or Cos of pitch Euler angle.
C6	Cos[XE(6)] or Cos of yaw Euler angle.
CT	Thrust coefficient.
DA1DU	Partial of longitudinal flapping to forward velocity (rad/ft/sec).
DB1DV	Partial of lateral flapping to side velocity (rad/ft/sec).
DC(i)	Control vector.
DC(1)	Main rotor collective pitch angle (rad).
DC(2)	Pitch control, B_1 , (rad).

DC(3) Roll control, A_1 , (rad).
 DC(4) Tail rotor collective pitch angle (rad).
 DENS.RATIO Density ratio.
 D.FUS Fuselage horizontal position of aerodynamic center (ft).
 D.FW Position of downwash on fuselage (ft).
 D.HT Horizontal tail aerodynamic center relative to c. g. (ft).
 D.HUB Hub horizontal position relative to c. g. (ft).
 DL.DB1 Direct flapping stiffness (rad/sec²).
 DL.DA1 Off-axis flapping stiffness (rad/sec²).
 D.TR Tail rotor horizontal position (ft).
 EPS.HT Downwash field on horizontal tail relative to induced velocity.
 F(i) Force and moment vector.
 F(1) Total x-force component (lb).
 F(2) Total y-force component (lb).
 F(3) Total z-force component (lb).
 F(4) Total rolling moment component (ft-lb).
 F(5) Total pitching moment component (ft-lb).
 F(6) Total yawing moment component (ft-lb).
 F(7) Pitch axis flapping angle, a_1 , (rad).
 F(8) Roll axis flapping angle, b_1 , (rad).
 FR.MR Effective frontal area of main rotor (ft²).
 FR.TR Effective frontal area of tail rotor (ft²).
 GAM.OM.16 One-sixteenth the product of Lock Number and rotor angular rate (rad/sec).
 GV(7) Longitudinal tip-path-plane angular rate (rad/sec).
 GV(8) Lateral tip-path-plane angular rate (rad/sec).
 H.FUS Fuselage vertical position of aerodynamic center relative to c. g. (ft).
 H.HUB Hub vertical position relative to c. g. (ft).
 H.TR Tail rotor vertical position relative to c. g. (ft).

HP.LOSS Net power loss due to transmission, accessories, etc.
 (hp).

IS Main rotor shaft incidence (rad).

ITB Inverse tip-path-plane lag (rad/sec).

ITB2.OM ITB squared over OMEGA.MR (rad/sec).

KC Flapping coupling factor.

KIND Induced velocity factor.

L.FUS Fuselage aerodynamic rolling moment (ft-lb).

L.MR Main rotor rolling moment (ft-lb).

L.TR Tail rotor rolling moment (ft-lb).

L.VT Vertical tail rolling moment (ft-lb).

M Vehicle mass (slug).

M.FUS Fuselage aerodynamic pitching moment (ft-lb).

M.HT Horizontal tail pitching moment (ft-lb).

M.MR Main rotor pitching moment (ft-lb).

M.WN Wing pitching moment (ft-lb).

N.FUS Fuselage aerodynamic yawing moment (ft-lb).

N.MR Main rotor yawing moment or torque (ft-lb).

N.TR Tail rotor yawing moment (ft-lb).

N.VT Vertical tail yawing moment (ft-lb).

OMEGA.MR Main rotor angular velocity (rad/sec).

OMEGA.TR Tail rotor angular velocity (rad/sec).

P.CLIMB Power loss due to change in potential energy (ft-
 lb/sec).

P.INDUCED.MR Power loss due to main rotor induced velocity (ft-
 lb/sec).

P.INDUCED.TR Power loss due to tail rotor induced velocity (ft-
 lb/sec).

P.PARASITE Power loss due to fuselage parasite drag (ft-
 lb/sec).

P.PROFILE.MR Power loss due to main rotor profile drag (ft-
 lb/sec).

POWER.FUS Power loss from fuselage aerodynamic drag (ft-
 lb/sec).

POWER.MR Power loss from main rotor and fuselage (ft-
 lb/sec).

VE(2) Y-axis velocity relative to earth (ft/sec).
 VE(3) Z-axis velocity relative to earth (ft/sec).
 VE(4) Roll-axis Euler angle rate (rad/sec).
 VE(5) Pitch-axis Euler angle rate (rad/sec).
 VE(6) Yaw-axis Euler angle rate (rad/sec).
 VG(1) X-gust component (ft/sec).
 VG(2) Y-gust component (ft/sec).
 VG(3) Z-gust component (ft/sec).
 VG(4) Inertial roll gust (rad/sec).
 VG(5) Inertial pitch-gust (rad/sec).
 VG(6) Inertial yaw-gust (rad/sec).
 VHAT.2 Intermediate variable in thrust calculations (ft²/sec²).
 VI.MR Main rotor induced velocity (ft/sec).
 VI.MR.2 VI.MR squared.
 VI.TR Tail rotor induced velocity (ft/sec).
 VI.TR.2 VI.TR squared.
 VP(i) Past value of VE(i).
 VR.TR Net vertical velocity relative to tail rotor blade (ft/sec).
 VB.TR Net vertical velocity through tail rotor actuator disk (ft/sec).
 VT Total airspeed (kt).
 VT.IN.FPS Total airspeed (ft/sec).
 VTA Total airspeed (ft/sec).
 V.TIP Main rotor tip speed (ft/sec).
 WA.FUS Apparent vertical velocity on fuselage (ft/sec).
 WB Net vertical velocity relative to rotor blade (ft/sec).
 WR Net vertical velocity through actuator disk (ft/sec).
 WT Gross weight (lb).
 XE(1) X-axis position (ft).
 XE(2) Y-axis position (ft).
 XE(3) Z-axis position (ft).
 XE(4) Roll Euler angle (rad).
 XE(5) Pitch Euler angle (rad).
 XE(6) Heading Euler angle (rad).

X.FUS Fuselage x-force (lb).
 X.GRAV Gravity x-force (lb).
 X.MR Main rotor x-force (lb).
 X.HT Horizontal tail x-force (lb).
 X.WN Wing x-force (lb).
 XU.U.FUS Fuselage parasite drag force (ft²).
 Y.FUS Fuselage y-force (lb).
 Y.GRAV Gravity y-force (lb).
 YMIN.VT Vertical tail stall factor (ft²).
 Y.MR Main rotor y-force (lb).
 Y.TRT Tail rotor y-force (lb).
 YUU.VT Vertical tail profile drag factor (ft²).
 YUV.VT Vertical tail circulation lift factor (ft²).
 Y.VT Vertical tail y-force (lb).
 YVV.FUS Fuselage sideward drag factor (ft²).
 ZMIN.HT Horizontal tail stall factor (ft²).
 ZMIN.WN Wing stall factor (ft²).
 Z.FUS Fuselage z-force (lb).
 Z.GRAV Gravity z-force (lb).
 Z.HT Horizontal tail z-force (lb).
 ZUU.HT Horizontal tail profile drag factor (ft²).
 ZUU.WN Wing profile drag factor (ft²).
 ZUW.HT Horizontal tail circulation lift factor (ft²).
 ZUW.WN Wing circulation lift factor (ft²).
 ZWW.FUS Fuselage quadratic drag coefficient along z-axis (ft²).

APPENDIX C
DEFINITION OF PROGRAM INPUT FILE

The following describes the input format needed to define the math model for a specific helicopter. The specific values given correspond to the AH-1S example. Individual entries are discussed in detail in Appendix D.

```

*****
*
*           DATA FILE FOR THE AH-S HELICOPTER PARAMETERS
*
*****

(CONFIGURATION, AIRCRAFT NAME, FS.CG, WL.CG,  WT,  IX,  IY,  IZ,  IXZ)
  102,           "AH-1S",   196   , 75   , 9000, 2593,14320,12330, 0

(FS.HUB, WL.HUB, IS, E.MR, I.B, R.MR, A.MR, RPM.MR, CDD, B.MR, C.MR, TWST.MR, K1)
  200 , 153 , 0 , 0 , 1382, 22, 6 , 324, 0.010, 2, 2.25, -.175, 0

(FS.FUS, WL.FUS, XU.FUS, YV.FUS, ZW.FUS)
  200, 65, -30 , -275, -41

(FS.WN, WL.WN, ZU.WN, ZW.WN, ZMAX.WN, B.WN)
  200, 65 , -39 , -161, -65, 10.75

(FS.HT, WL.HT, ZU.HT, ZW.HT, ZMAX.HT)
  400, 65, 0 , -80, -32

(FS.VT, WL.VT, YU.VT, YV.VT, YMAX.VT)
  490, 80, 0 , -62, -50

(FS.TR, WL.TR, R.TR, A.TR, SOL.TR, RPM.TR, TWST.TR)
  521.5, 119, 4.25, 6, .105, 1660, 0

```

APPENDIX D
MATH MODEL MATCHING PROCESS FOR AUGUSTA A109 II HELICOPTER

This appendix describes a minimum-complexity math model version of the Augusta A109 II helicopter based on available flight data and flight manual information. The data were furnished by the Army Aeroflightdynamics Directorate in order to provide an illustration of the parameter matching procedure and verification of the resulting math model.

It is believed that the results of this modeling process are sufficiently good to be used as the basis of a lateral control handling qualities experiment such as that performed under this contract.

The general procedure followed was first to quantify the basic math model form using engineering data provided by the helicopter manufacturer. The second step was to adjust parameters in order to match trim data from flight and to add certain nonlinear characteristics such as downwash on tail and fuselage. The final step was to match dynamic response cases adjusting rotor model parameters. Details of the matching procedure are presented below.

1. Initial Quantification of Model Parameters

The first step was to set up the main data file for the math model using all available engineering data. In this case a fairly complete array of these data were supplied by the manufacturer. The following paragraphs present the initial quantification of parameters for each of the model components and a short discussion of the basis for quantification.

Loading Parameters

FS.CG,	WL.CG,	WT
132.7 in ,	38.5 in ,	5401 lb

"FS.CG" is the location of the center of gravity in the fuselage reference system in inches from the zero fuselage station. For the A109 this can be found in the flight manual but must be converted from millimeters.

"WL.CG" is the vertical center of gravity location in inches above the zero waterline. Without a specific value, this can be estimated as approximately at the level of the engine. However it is important to determine this quantity as accurately as possible since a significant portion of flapping stiffness (thus

pitch and roll damping) results from the vertical offset of the rotor hub from the vertical center of gravity.

"WT" is the gross weight of the aircraft in pounds. A representative value can be picked from the flight manual loading envelope diagram, however a fairly accurate weight should be available for any given set of flight data.

IX,	IY,	IZ,	IXZ
1590 slug-ft ² ,	6761 slug-ft ² ,	6407 slug-ft ² ,	598 slug-ft ²

"IX," "IY," "IZ," and "IXZ" are the moments of inertia about the center of gravity in the "body" or fuselage reference line axis system. The first three are essential to the math model. IXZ can be neglected but an effect can be seen in yaw response due to roll axis inputs. It should be recognized that moments of inertia often cannot be measured accurately and can therefore be subject to modification in order to match flight data. For the A109 the value of IX was reduced from that shown above in order to match the primary roll damping mode.

Main Rotor Parameters

FS.HUB,	WL.HUB,	IS,	E.MR,	I.B,
132.4 in,	98.2 in,	.11 rad,	0.5 ft,	212 slug-ft ²

"FS.HUB" is the fuselage reference system location of the main rotor hub measured aft of the zero fuselage station.

"WL.HUB" is the corresponding waterline location of the main rotor hub.

"IS" is the main rotor shaft tilt forward of vertical in the fuselage reference system and measured in radians.

"E.MR" is the geometric main rotor flapping hinge offset for an articulated rotor or the effective hinge offset for a rigid rotor. Any empirical adjustment of this parameter should be done with care. In general, for teetering and articulated hubs, variation of the roll moment of inertia is probably easier to justify than the geometric flapping hinge offset.

"I.B" is the flapping inertia of a single blade about the flapping hinge.

R.MR, A.MR, RPM.MR, CDO, B.MR,
 18 ft, 6/rad , 385 rpm, 0.010, 4 blades

"R.MR" is the actual main rotor diameter in ft.

"A.MR" is the effective lift-curve-slope of the main rotor in units of non-dimensional lift coefficient per unit radian of angle of attack. Values of 5.7 or 6 are commonly used.

"RPM.MR" is the nominal angular velocity of the main rotor in units of revolutions per minute. This can ordinarily be found in a flight manual.

"CDO" is the effective profile drag for the main rotor blade cross section. Values of 0.010 or 0.012 are commonly used, but this can be adjusted in order to fit power required data, especially in hovering flight.

"B.MR" is the number of blades in the main rotor array.

C.MR, TWST.MR, K1
 1.10 ft, -.105 rad, .096

"C.MR" is the blade chord in ft.

"TWST.MR" is the effective blade twist in radians.

"K1" is the tangent of delta-3, the effective pitch-flap coupling based on flapping hinge geometry. Although the above value was given for the A109, the effect was ultimately neglected in matching pitch and roll cross-coupling effects.

Fuselage Parameters

FS.FUS, WL.FUS, XUU.FUS, YVV.FUS, ZWW.FUS
 132 in, 38 in, -10.8 ft², -167 ft², -85 ft²

"FS.FUS" is the fuselage station corresponding to the effective center of pressure in the vertical axis. Here it was nominally set equal to the main rotor hub position.

"WL.FUS" is the waterline for the center of pressure in the longitudinal axis. It can be adjusted to account for hub drag as well as that of the fuselage itself. In this case it was set at the vertical center of gravity.

"XUU.FUS" is the effective frontal area corresponding to profile drag in the x-axis. The value used here was provided by the manufacturer.

"YVV.FUS" is the effective side area for sideward flight, that is, sideslip equal to 90 deg. Again it was provided by the manufacturer.

"ZWW.FUS" is the effective planview area for vertical flight, i. r., angle of attack equal to 90 deg. It affects the power required to hover and is used in conjunction with pitching moment due to airspeed changes.

Wing Parameters

FS.WN, WL.WN, ZUU.WN, ZUW.WN, ZMAX.WN, B.WN

000 in, 00 in, 000 ft², 0000 ft², 000 ft², 1 ft

The A109 does not have a wing, thus zeros were set for all values except the span which needs any arbitrary non-zero value to avoid division by zero. All the individual values can however be found or estimated similarly to those for the horizontal tail.

Horizontal Tail Parameters

FS.HT, WL.HT, ZUU.HT, ZUW.HT, ZMAX.HT

330 in, 54 in, .4 ft², -34 ft², -22 ft²

"FS.HT" is the effective aerodynamic center of the horizontal tail in inches from the reference fuselage station. It can be estimated as the quarter mean aerodynamic chord based on engineering data or on a planview of the aircraft.

"WL.HT" is the effective vertical location of the horizontal tail. The value used is important in computing the position of the main rotor downwash field as airspeed is varied.

"ZUU.HT" is the effective lift per unit dynamic pressure at zero angle of attack relative to the fuselage reference system. The value used is important in establishing the trim pitch angle at high forward velocities.

"ZUW.HT" is the effective variation in circulation lift and can be estimated as the negative product of lift-curve-slope and surface area.

Vertical Fin Parameters

FS.VT, WL.VT, YUU.VT, YUV.VT, YMAX.VT

380 in, 80 in, 3.3 ft², -47 ft², -17 ft²

"FS.VT" is the fuselage station for the effective aerodynamic center of the vertical fin.

"WL.VT" is the vertical position of the vertical fin aerodynamic center.

"YUU.VT" is the net y-force per unit dynamic pressure for zero sideslip. This arises either from vertical fin camber or incidence.

"YUV.VT" is the sideforce arising from a side-velocity component and is approximately equal to the lift-curve slope time the net fin area.

"YMAX.VT" sets the maximum sideforce generated by the vertical tail at stall.

Tail Rotor Parameters

FS.TR, WL.TR, R.TR, A.TR, SOL.TR, RPM.TR, TWST.TR

391 in, 70 in, 3.1 ft, 3/rad, .134, 2080 rpm, -.137 rad

"FS.TR" and "WL.TR" represent the center of the tail rotor hub in the fuselage reference system.

"R.TR" is the radius of the tail rotor in ft.

"A.TR" is the effective lift-curve-slope of the tail rotor and can be set equal to that of the main rotor. It can be adjusted downward in order to account for interference effects with the vertical fin. In this case it was reduced by one half in order to match pedal trim data as discussed below.

"SOL.TR" is the solidity of the tail rotor, i. e., the ratio of actual blade area to disk area.

"RPM.TR" is the angular velocity of the tail rotor in terms of revolutions per minute.

"TWST.TR" is the effective twist of the tail rotor blade.

2. Model Adjustments Needed to Match Static Trim Data

Several model parameters and functions were adjusted in order to produce good static trim matches. This was important in establishing realistic attitudes, control deflections, and power requirements.

For the A109 those adjustments found necessary included:

- o A tail rotor efficiency factor of 0.5 in order to account for vertical fin interference effects.
- o A triangular main rotor downwash field superimposed on the horizontal tail vertical velocity and displaced 1 ft rearward.
- o A magnification of the dihedral effect at low speeds individually set for the lateral and longitudinal axes.
- o A shift in the planview center of pressure such that the downwash on the fuselage provides a pitching moment proportional to airspeed.

Tail Rotor Effectiveness

The first adjustment was made by changing "A.TR" from a nominal value of 6/rad to 3/rad. This was done on the basis of matching the pedal deflection (i. e., tail rotor collective pitch), especially at low speed and hover. The effect was applied directly in the tail rotor thrust equation wherein "A.TR" appears.

$$\text{THRUST.TR} = (\text{VB.TR} - \text{VI.TR}) \\ * \text{OMEGA.TR} * \text{R.TR} * \text{RHO} * \text{A.TR} * \text{SOL.TR} * \text{PI} * \text{R.TR} * \text{R.TR} / 4$$

Triangular Induced-Velocity Field

The second adjustment consisted of assuming a triangular induced velocity field with a magnitude of 2 at the rotor tip and zero at the hub. This can be justified by observing measured downwash field data such as presented by Heyson and Katzoff in NACA Report 1319. This effect is crucial to portraying the large change in pitch attitude between zero airspeed and 20 kt rearward. The program instructions affected are given below:

$$\text{D.DW} = (\text{VA}(1) / (\text{VI.MR} - \text{VA} * 3) * (\text{H.HUB} - \text{H.HT})) - (\text{D.HT} - \text{D.HUB} - \text{R.MR})$$

(position where edge of downwash passes through plane of horizontal tail)

D.DW=D.DW + 1

(shift of D.DW by one foot in order to match speed where downwash on tail effect is seen in trim data)

IF (D.DW>0 AND D.DW<R.MR) THEN EPS.HT= 2*(1-D.DW/R.MR)
ELSE EPS.HT=0

(triangular downwash if D.DW is negative)

WA.HT = VA(3) - EPS.HT*VI.MR + D.HT*VA(5) : ' local z-vel at h.t.
(appearance of downwash effect in computation of relative z-velocity component at horizontal tail)

Dihedral Magnification at Low Speed

The third adjustment consisted of magnifying the effective dihedral effect at very low speeds when the rotor wake interacts with the fuselage. This enhanced dihedral effect could be seen directly in the cyclic control gradient with respect to forward speed and side velocity.

The model equations affected are limited to the rotor flapping equations. Below a speed of VTRANS the computed parameters da1du and db1dv are multiplied by 3 and 2, respectively. The values are empirical and based on cyclic trim data. VTRANS was set at 30 kt based on the large change in stick trim observed at that point. The program statements involved are shown below:

IF VA(1) < VTRANS THEN WAKE.FN = 1 ELSE WAKE.FN = 0
(rotor wake effects are added to the effective tip-path-plane dihedral when WAKE.FN = 1, i. e., below and airspeed equal to VTRANS)

A.SUM = GV(8)-DC(2)+KC*GV(7)+DB1DV*VA(2)*(1+WAKE.FN)
(i. e., b1 - A1 + e.a1 + db1/dv .V)

B.SUM = GV(7)+DC(3)-KC*GV(8)+DA1DU*VA(1)*(1+2*WAKE.FN)
(i. e., a1 + B1 - e.b1 + da1/du .U)

GR(7)= - ITB*B.SUM - ITB2.OM*A.SUM - VA(5)
(i. e., a1.dot = ...)

GR(8)= - ITB*A.SUM + ITB2.OM*B.SUM - VA(4)
(i. e., b1.dot = ...)

Downwash Center of Pressure on Fuselage

The fourth and final adjustment needed to match trim data is the shift of downwash center of pressure on the fuselage as speed varies. This affects not only the longitudinal cyclic to trim but also the trim pitch attitude.

The approach was to compute an effective wake position in the plane of the fuselage similar to that computed for the horizontal tail. This position was then used in the pitching moment equation along with an empirical magnification factor. The net effect is a change in fuselage pitching moment with forward speed.

The program instructions affected are:

WA.FUS = VA(3) - VI.MR
(computed net downwash on fuselage, i. e., $W - V_i$)

D.FW=(VA(1)/(-WA.FUS)*(H.HUB-H.FUS))-(D.FUS-D.HUB)
(computed position of downwash at fuselage waterline as airspeed varies)

D.FW=3*D.FW
(empirical magnification of a.c. shift used to match trim data)

Z.FUS = R2 * ZWW.FUS * ABS(WA.FUS) * WA.FUS
(z-force resulting from downwash on fuselage)

M.FUS = Z.FUS * D.FW - X.FUS * H.FUS
(pitching moment due to x- and z-forces acting at their respective aerodynamic centers)

The resulting math model trim characteristics are compared with the A109 flight data in the following pages.

Model 100-1

CONTROLLABILITY

Helicopter: A109K

S/N : 7310

G.W.(Kg): 2450

Flight N° :

Date:

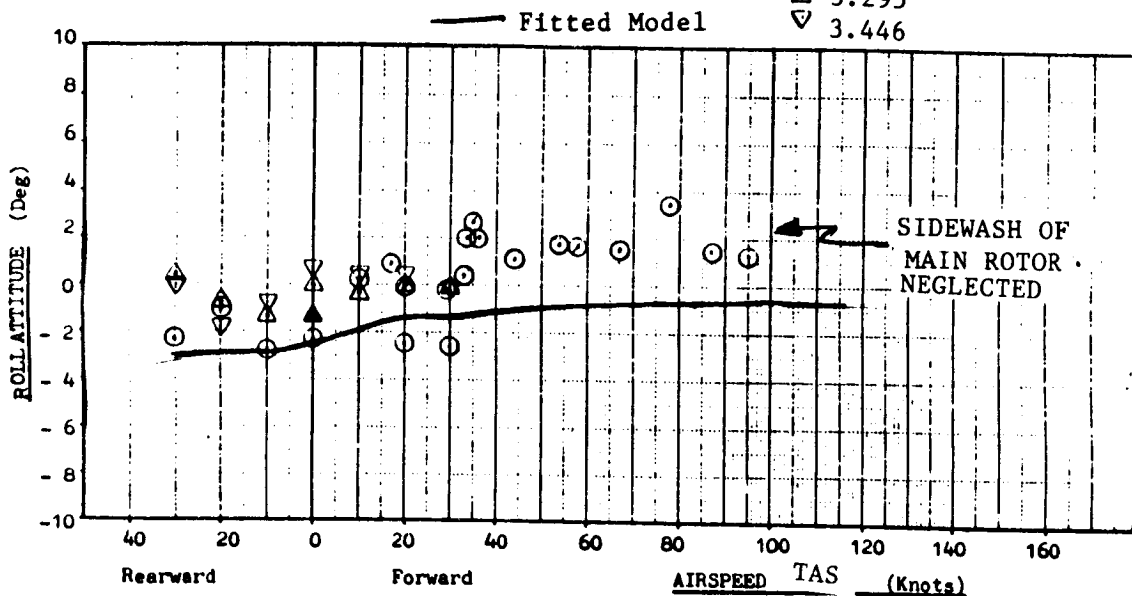
Press.Alt.(Ft):

Configuration:

C.G. Sta. (m) : ○ 3.370

△ 3.295

▽ 3.446



DATA 3

PAGE

Model 100-1

CONTROLLABILITY AND CONTROL MARGIN

Helicopter: A109K^t

S/N : 7310

G.W.(Kg): 2450

Flight N° :

Date:

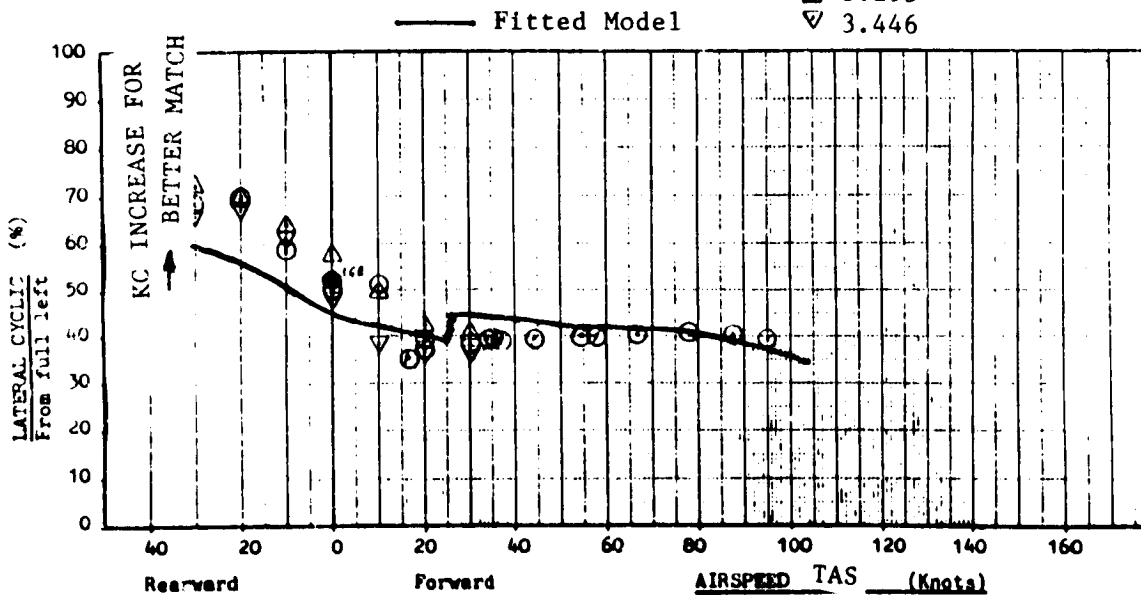
Press.Alt.(Ft):

Configuration:

C.G. Sta. (m) : ○ 3.370

△ 3.295

▽ 3.446



DATA 3

PAGE

Helicopter: A109K

S/N : 7310

G.W.(Kg): 2450

Flight N° :

Date:

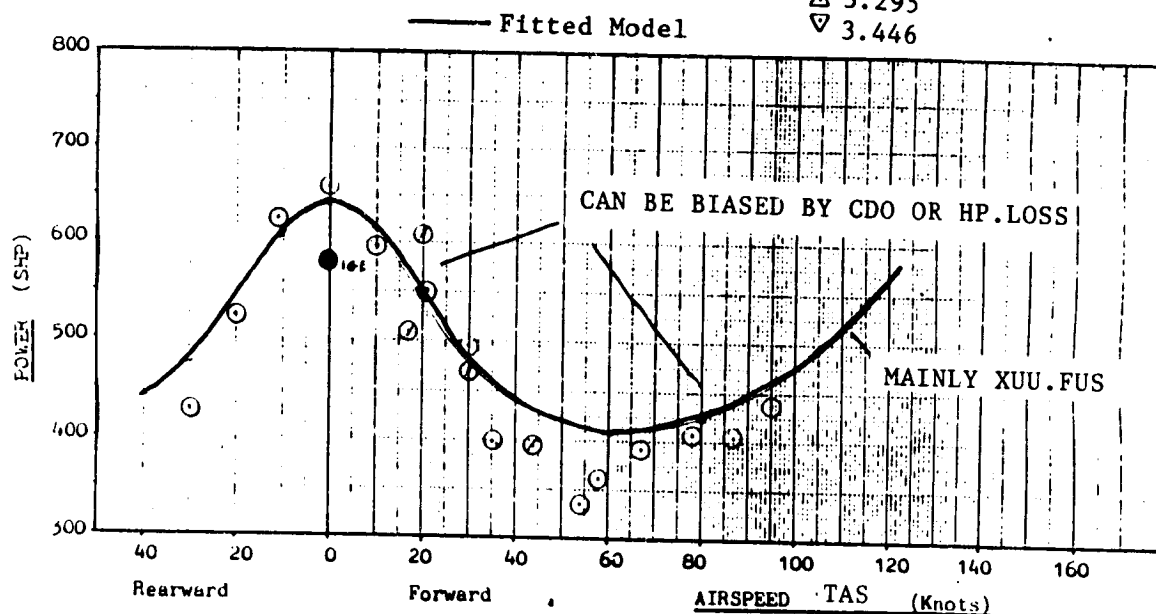
Press.Alt.(Ft):

Configuration:

C.G. Sta. (m) : \odot 3.370

\triangle 3.295

∇ 3.446



ORIGINAL PAGE IS
OF POOR QUALITY

CONTROLLABILITY AND CONTROL MARGIN

Helicopter: A109K

S/N : 7310

G.W.(Kg): 2450

Flight N° :

Date:

Press.Alt.(Pt):

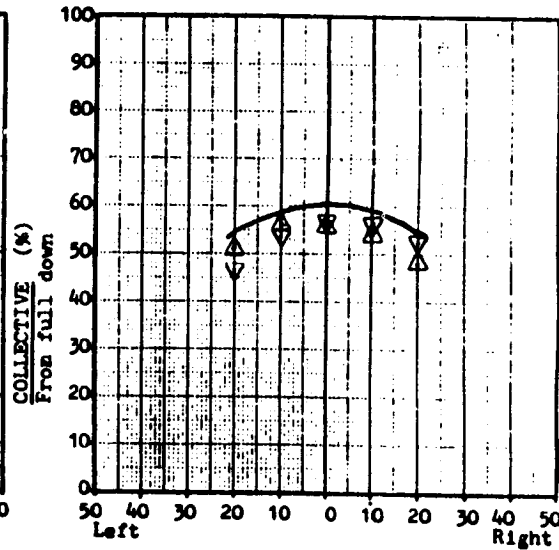
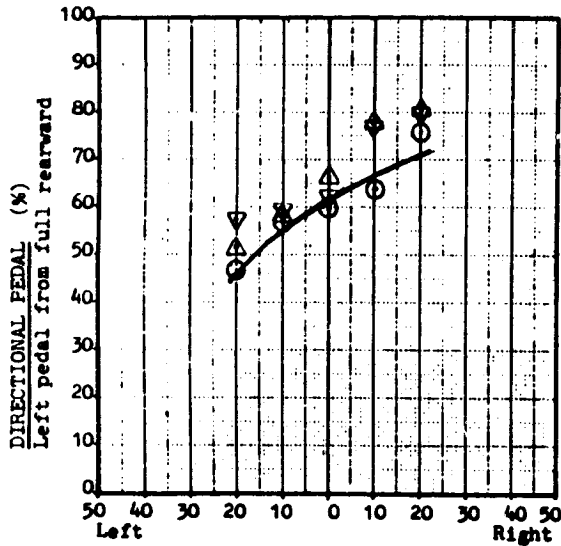
Configuration:

C.G. Sta. (m) : \odot 3.370

\triangle 3.295

∇ 3.446

— Fitted Model



AIRSPEED - TAS - (Knots)

N°
DATA
PAGE

ORIGINAL PAGE IS
OF POOR QUALITY

3. Model Adjustments Needed to Match Dynamic Response Data.

The final step in the model matching process was the adjustment in the model to account for features seen in both the primary on-axis response as well as cross-coupling effects.

The adjustment of dynamic response features was limited only to pitch and roll response in hover. Other axes and flight conditions would be addressed in a similar manner.

In the case of the A109 it was found that by removing cross-coupling in flapping and hub moment equations a reasonably good match could be achieved for the pitch and roll axes with only minor adjustment of moments of inertia.

Roll Inertia Reduction

The dominant roll-damping mode was matched closely by varying the lateral flapping stiffness via a reduction in the roll moment of inertia. This was considered preferable to increasing the flapping hinge offset since the latter would also affect the pitch response.

The value of IX in the data input file was reduced from 1590 to 1300 slug-ft².

Removal of Rotor Flap Cross-Coupling

One element of pitch response due to a roll input can be attributed to the cross-coupling in the rotor flapping equations. In this case it was found that decoupled flapping provided a better match to flight data thus the simplification was made.

The coupled first-order flap equations were decoupled by simply by recomputing the values of "ITB" and "ITB2.OM." Thus the primary flapping response consists only of a first-order lag as described in Reference 1.

This change is accomplished by setting:

ITB = GAM.OM.16

and ITB2.OM = 0

Elimination of Hub-Moment Cross-Coupling

The aerodynamic cross-coupling represented by DL.DA1 was also set equal to zero in order to further suppress pitch cross-coupling due to roll as seen in flight data.

Removal of Delta-3 Effect

In order to maintain consistency of model complexity following the above simplifications, the Delta-3 effect as represented by the parameter "K1" was also set to zero.

Adjustment of Cross-Axis Inertia

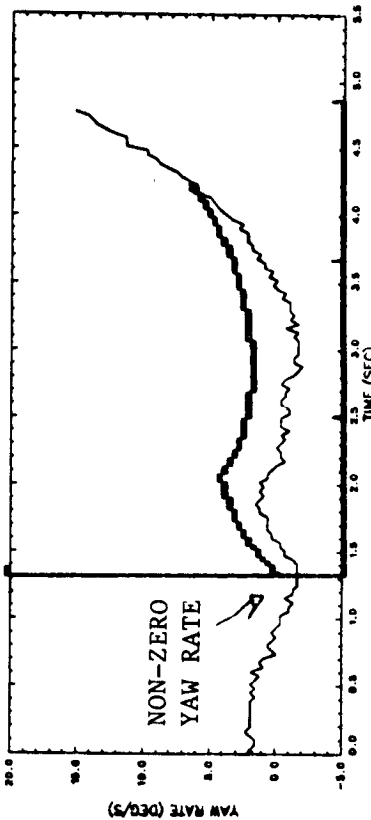
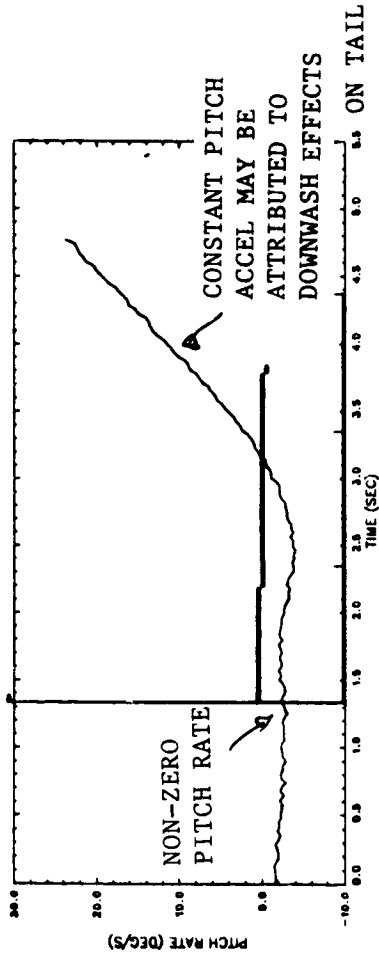
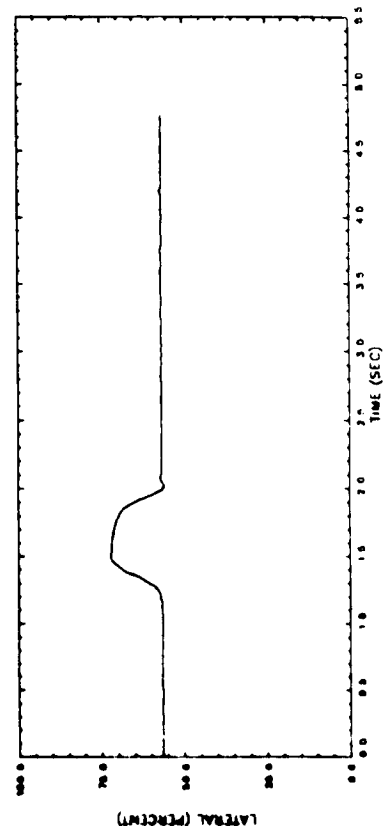
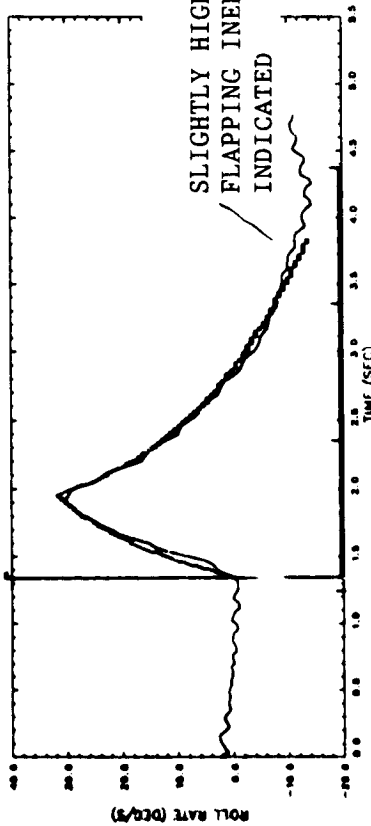
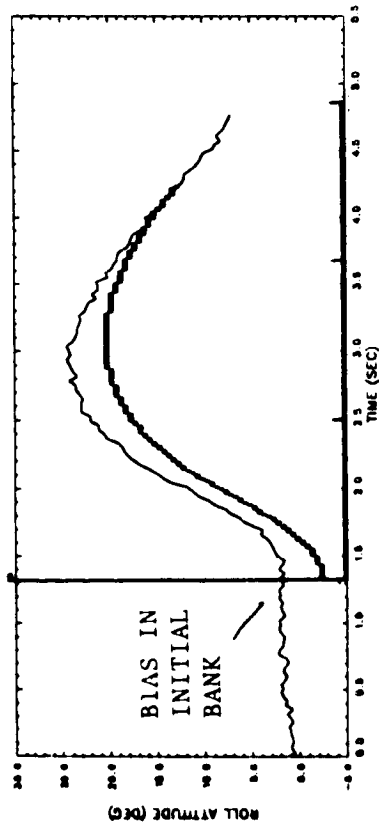
The effect of an inclined principal axis of inertia could be seen readily in the short-term yaw response following a roll input. An increase in I_{xz} from 598 to 800 slug-ft² provided a slightly better match to flight data.

Adjustment of Cyclic Control Phasing

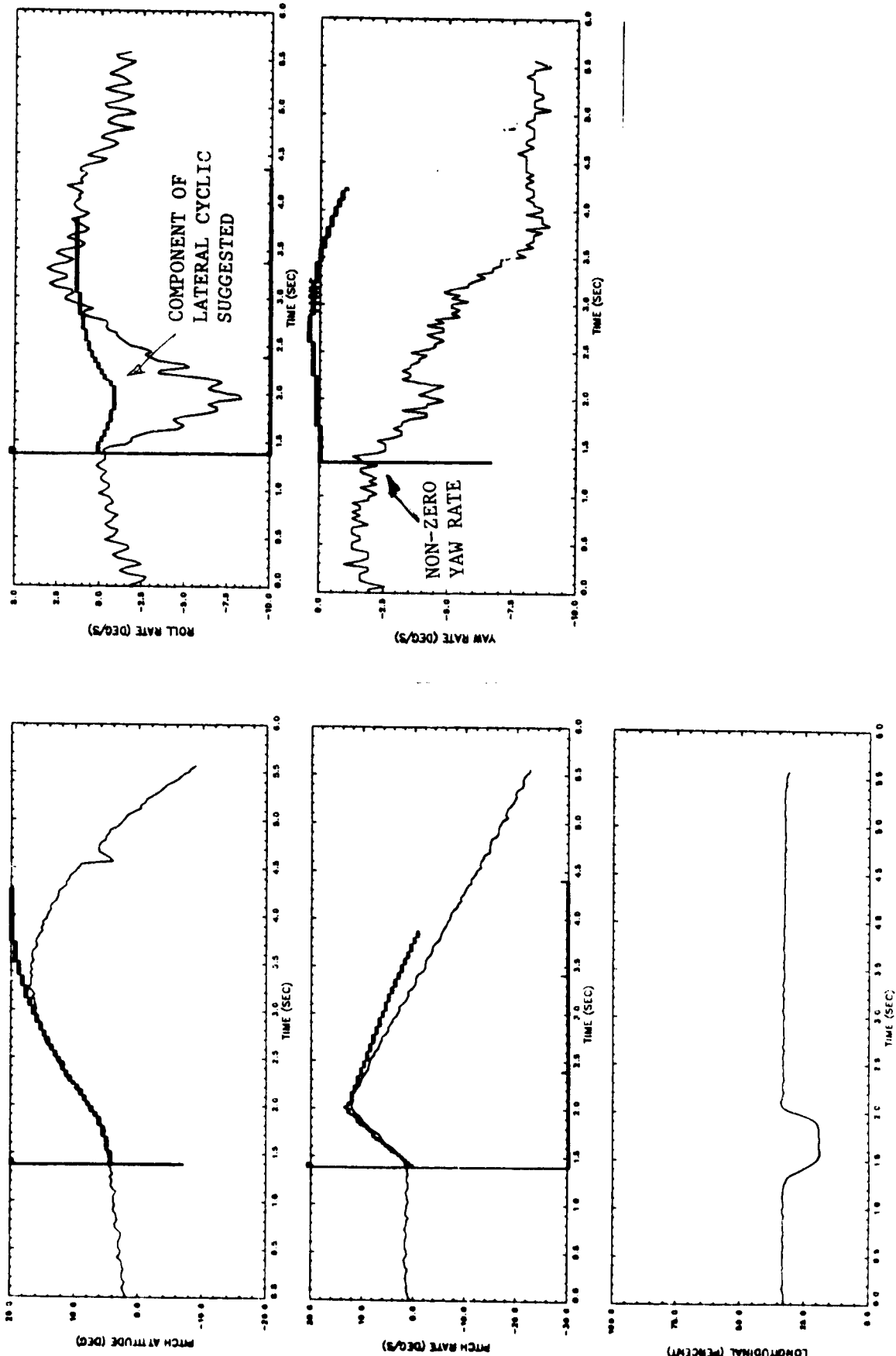
There was some evidence of cyclic control phasing in the A109 although control system geometry indicated none. First, inspection of swashplate angle records for pitch and roll inputs showed minor off-axis inputs which were generally consistent with the cross-coupling response which followed. Also there was a direct measurement of a nearly 10 deg steady lead-lag component which, depending upon the hub pitch control geometry, could contribute to a cyclic control phase effect.

The results of the dynamic response adjustments for pitch and roll inputs in hover are shown in the following pages.

FLT 156 #33, HOVER, LATERAL RIGHT PULSE



FLT 156 #31, HOVER, LONG AFT PULSE



4. Revised Program Listings for the A109 Math Model

The following listings show the revisions made to the data file, preliminary calculations, and the dynamics subroutine.

Input Data File

```
type HEL302.DAT
]*****
*
*          DATA FILE FOR THE A109 II HELICOPTER PARAMETERS          *
*
******

(CONFIGURATION, AIRCRAFT NAME, FS.CG, WL.CG, WT, IX, IY, IZ, IXZ)
302,      "A109 II", 132.7 , 38.5 , 5401, 1300, 6760, 6407, 800

(FS.HUB, WL.HUB, IS, E.MR, I.B, R.MR, A.MR, RPM.MR, CDD, B.MR, C.MR, TWST.MR, K1)
132.4, 98.2, .11, 0.50, 212, 18, 6 , 385, 0.010, 4, 1.10, -.105, 0

(FS.FUS, WL.FUS, XU.FUS, YV.FUS, ZW.FUS)
132,    38,   -10.8,   -167,   -85

(FS.WN, WL.WN, ZUU.WN, ZUM.WN, ZMAX.WN, B.WN)
0 , 0 , 0 , 0 , 0 , 1

(FS.HT, WL.HT, ZUU.HT, ZUM.HT, ZMAX.HT)
330, 54, .4, -34, -22

(FS.VT, WL.VT, YUU.VT, YUV.VT, YMAX.VT)
380, 80, 3.3, -47, -17

(FS.TR, WL.TR, R.TR, A.TR, SOL.TR, RPM.TR, TWST.TR)
391, 70, 3.1, 3, .134, 2080, -.137
```

C)

Preliminary Calculations

```

1490 *****
1500
1510 Preliminary Calculations
1520
1530 *****
1540
1550 VT.IN.FPS = ABS(XDOT/COS(GAMMA.RAD))
1560 VT = VT.IN.FPS/FPS.PER.KNOT
1570 VT.IN.FPS.SQUARED = VT.IN.FPS ^ 2
1580 M = WT/GRAV
1590 OMEGA.MR = RPM.MR*2*PI/60
1600 OMEGA.TR = RPM.TR*2*PI/60
1605 V.TIP=R.MR*OMEGA.MR
1610 FR.MR = CDO*R.MR*B.MR*C.MR
1620 FR.TR = CDO*R.TR*B.TR*C.TR
1630 HP.LOSS = 90
1640 VTRANS = 50 : speed for transition from dihedral wake function
1660 TEMP.RATIO=1! - LAPSE.RT*H
1670 PRESS.RATIO = TEMP.RATIO^TEMP.EXP
1680 DENS.RATIO = PRESS.RATIO/TEMP.RATIO
1685 R0 = DENS.RATIO*RHO.SEA.LEVEL : R2=R0/2
1688 GAM.DM.16 = R0*A.MR*C.MR*R.MR^4/I.B *OMEGA.MR/16*(1+8/3*E.MR/R.MR)
1690 KC = (.75*OMEGA.MR*E.MR/R.MR / GAM.DM.16 ) + K1: flapping aero cpl
1691 ITB2.DM = OMEGA.MR/(1+(OMEGA.MR/GAM.DM.16)^2) : flapping x-cpl coef
1692 ITB = ITB2.DM*OMEGA.MR/GAM.DM.16 : flapping primary resp
1693 ITB2.DM = 0 :ITB = GAM.DM.16 : temp mod for A109
1694 DL.DB1 = B.MR/2*(1.5*I.B*E.MR/R.MR*OMEGA.MR*OMEGA.MR) : primary flapping stiffness
1696 DL.DA1=R2*A.MR*B.MR*C.MR*R.MR*V.TIP*V.TIP*E.MR/6: cross flapping stiffness
1697 CT=WT/(R0*PI*R.MR*R.MR*V.TIP*V.TIP) : thrust coefficient
1698 A.SIGMA=A.MR*B.MR*C.MR/R.MR/PI : a x sigma
1699 DB1DV=2/OMEGA.MR/R.MR*(8*CT/A.SIGMA+(SQR(CT/2))): TPP dihedral effect
1700 DA1DU=-DB1DV : TPP pitchup with speed
1702
1730 H.HUB = (WL.HUB-WL.CG)/12 : D.HUB = (FS.HUB-FS.CG)/12 : hub re cg
1740 H.FUS = (WL.FUS-WL.CG)/12 : D.FUS = (FS.FUS-FS.CG)/12 : fuselage re cg
1750 H.WN = (WL.WN -WL.CG)/12 : D.WN = (FS.WN -FS.CG)/12 : wing re cg
1760 H.HT = (WL.HT -WL.CG)/12 : D.HT = (FS.HT -FS.CG)/12 : horizontal tail re cg
1770 H.VT = (WL.VT -WL.CG)/12 : D.VT = (FS.VT -FS.CG)/12 : vertical fin re cg
1780 H.TR = (WL.TR -WL.CG)/12 : D.TR = (FS.TR -FS.CG)/12 : tail rotor re cg
1790
1800 RETURN

```

ORIGINAL PAGE IS
OF POOR QUALITY

Dynamics Subroutine

ORIGINAL PAGE IS
OF POOR QUALITY

```

6000 *****
6010
6020 DYNAMICS: Dynamics subroutine
6030
6040 *****
6070
6080 IF CHECK = 1 THEN GOSUB 11940 : ' print state variable to screen
6090
6100 ***** Preliminary calculations *****
6120
6130 C4 = COS(XE(4)) : S4 = SIN(XE(4)) : ' evaluate Euler angle trig fns
6140 C5 = COS(XE(5)) : S5 = SIN(XE(5))
6160
6170 VA(1)=VB(1) : ' -(V6(1)*C5) : ' evaluate relative air mass velocities
6180 VA(2)=VB(2) : ' -(V6(2)*C6-V6(1)*S6)
6190 VA(3)=VB(3) : ' -(V6(3)*C5+V6(1)*S5)
6200 VA(4)=VB(4) : ' -V6(4)
6210 VA(5)=VB(5)
6220 VA(6)=VB(6)
6230
6290 VTA=SQR(VA(1)*VA(1)+VA(2)*VA(2)+VA(3)*VA(3))
6320
6330 ***** Rotor tip path plane dynamics *****
6340
6341 IF VA(1) < VTRANS THEN MAKE.FN = 1 ELSE MAKE.FN = 0 : ' rotor wake effects
6345 A.SUM= 6V(8)-DC(2)+KC+6V(7)+DB1DV*VA(2)*(1+MAKE.FN) : ' b1 - A1 + e.a1 + db1/dv .V
6346 B.SUM= 6V(7)+DC(3)-KC+6V(8)+DA1DU*VA(1)*(1+2*MAKE.FN) : ' a1 + B1 - e.b1 + da1/du .U
6347
6350 GR(7)= - ITB*B.SUM - ITB2.OM*A.SUM - VA(5) : ' a1.dot
6360 GR(8)= - ITB*A.SUM + ITB2.OM*B.SUM - VA(4) : ' b1.dot
6370
6380 6V(7)=6V(7) + ST*(A2*GR(7) + B2*AP(7)) : ' a1 updated
6390 6V(8)=6V(8) + ST*(A2*GR(8) + B2*AP(8)) : ' b1 updated
6400
6410 AP(7)=GR(7) : AP(8)=GR(8) : ' save past values
6420
6430 ***** Main Rotor thrust and induced velocity *****
6440
6490 MR = VA(3) + (6V(7) - IS)*VA(1) - 6V(8)*VA(2) : ' z-axis vel re rotor plane
6500 NB = MR + 2/3*OMEGA.MR*R.MR*(DC(1) + .75*TWST.MR) : ' z-axis vel re blade
6510
6540 FOR I=1 TO 5 : ' iterative solution of thrust and induced vel
6550 THRUST.MR=(NB-VI.MR)*OMEGA.MR*R.MR*(RHO*A.MR*B.MR*C.MR/R.MR/4
6570 VHAT.2=VA(1)^2 + VA(2)^2 + MR*(MR-2*VI.MR)
6580 VI.MR.2=SQR((VHAT.2/2)*(VHAT.2/2)+(THRUST.MR/2/(RHO*PI*R.MR^2))^2) - VHAT.2/2
6590 VI.MR=SQR(ABS(VI.MR.2)) : ' main rotor induced velocity
6610 NEXT I
6620

```

02

```

6630 ***** Fuselage *****
6640
6650 MA.FUS = VA(3) - VI.MR      : include rotor downwash on fuselage
6652 D.FW=( VA(1)/(-MA.FUS)*(H.HUB-H.FUS) )-( D.FUS-D.HUB ) : position of downwash on fuselage
6653 D.FW=3*D.FW      : empirical correction for fus a.c. shift magnification
6660
6670 X.FUS = R2 * XU.FUS + ABS(VA(1)) * VA(1)  : drag force
6680 Y.FUS = R2 * YV.FUS + ABS(VA(2)) * VA(2)  : side-force
6690 Z.FUS = R2 * ZW.FUS + ABS(MA.FUS) * MA.FUS : heave force
6710 L.FUS = Y.FUS*H.FUS
6720 M.FUS = Z.FUS*D.FW - X.FUS*H.FUS
6740
6780 P.INDUCED.MR = THRUST.MR * VI.MR
6790 P.CLIMB = WT*HDDT
6800 P.PARASITE = - X.FUS*VA(1) - Y.FUS*VA(2) - Z.FUS*MA.FUS
6810 P.PROFILE.MR = R2*(FR.MR/4)*OMEGA.MR*R.MR*(OMEGA.MR^2*R.MR^2 + 4.6*(VA(1)*VA(1)+VA(2)*VA(2)))
6820 POWER.MR = P.INDUCED.MR + P.CLIMB + P.PARASITE + P.PROFILE.MR
6830 POWER.ROTOR.MR = P.INDUCED.MR + P.PROFILE.MR
6840 POWER.FUS = P.PARASITE
6850 TORQUE.MR = POWER.MR/OMEGA.MR
6860
6870 Compute main rotor force and moment components.
6880
6890 X.MR = -THRUST.MR * (GV(7)-IS)
6900 Y.MR = THRUST.MR * GV(8)
6910 Z.MR = -THRUST.MR
6920 L.MR = Y.MR*H.HUB + DL.DB1*GV(8) + DL.DA1*(GV(7)+DC(3) - K1*GV(6))
6970 M.MR = Z.MR*D.HUB - X.MR*H.HUB + DL.DB1*GV(7) +DL.DA1*(-GV(8)+DC(2) - K1*GV(7))
6980 N.MR = TORQUE.MR
6990
7000 ***** Tail Rotor thrust and induced velocity *****
7010
7060 VR.TR = -(VA(2) - VA(6)*D.TR + VA(4)*H.TR) : velocity relative to rotor plane
7070 VB.TR = VR.TR +2/3*OMEGA.TR*R.TR*(DC(4)+TWST.TR*.75) : velocity relative to blade
7100
7110 FOR I=1 TO 5      : iterate on thrust and induced velocity
7120   THRUST.TR=(VB.TR-VI.TR)*OMEGA.TR*R.TR*RHO*A.TR*SOL.TR*PI*R.TR*R.TR/4
7140   VHAT.2=(VA(3)+VA(5)*D.TR)^2 + VA(1)^2 + VR.TR*(VR.TR-2*VI.TR)
7150   VI.TR.2=SQR((VHAT.2/2)*(VHAT.2/2)+(THRUST.TR/2/(RHO*PI*R.TR^2))^2) - VHAT.2/2
7160   VI.TR=SQR(ABS(VI.TR.2))
7180 NEXT I
7190
7220 POWER.TR = THRUST.TR*VI.TR
7290 Y.TR = THRUST.TR
7310 L.TR = Y.TR*H.TR
7330 N.TR = -Y.TR*D.TR
7340
7360 ***** Horizontal tail *****
7370
7410 D.DN=( VA(1)/(VI.MR-VA*3)*(H.HUB-H.HT) )-( D.HT-D.HUB-R.MR ) : impingement of downwash on tail?
7411 D.DN=D.DN + 1      : shifts transition position for empirical correction
7415 EPS.HT=.5*(1+SGN(D.DN)) : uniform downwash field
7416 IF (D.DN>0 AND D.DN<R.MR) THEN EPS.HT= 2*(1-D.DN/R.MR) ELSE EPS.HT=0 : triangular downwash field
7440
7450 MA.HT = VA(3) - EPS.HT*VI.MR + D.HT*VA(5) : local z-vel at h.t.
7455 VTA.HI=SQR(VA(1)+VA(1)+VA(2)+VA(2)+MA.HT*MA.HT)
7460 Z.HT=R2*(ZUU.HT*ABS(VA(1))*VA(1) + ZUW.HT*ABS(VA(1))*MA.HT) : circulation lift on h.t.
7470
7500 IF ABS(MA.HT)>.3*ABS(VA(1)) THEN Z.HT=R2*ZMAX.HT*ABS(VTA.HI)*MA.HT : surface stalled?
7530

```

```

7560 M.HT = Z.HT*D.HT : ' pitching moment
7570
7590 ***** Wing *****
7600
7640 WA.WN = VA(3) -VI.MR : ' local z-vel at wing
7650 VTA.WN =SQR(VA(1)*VA(1)+WA.WN*WA.WN)
7660
7670 Z.WN=R2*(ZUU.WN*VA(1)*VA(1) + ZUM.WN*VA(1)*WA.WN) : ' normal force
7680 X.WN=-R2/PI/VTA.WN/VTA.WN*(ZUU.WN*VA(1)*VA(1)+ZUM.WN*VA(1)*WA.WN)^2 : ' induced drag
7690
7720 IF ABS(WA.WN)>.3*ABS(VA(1)) THEN Z.WN=R2*ZMAX.WN*ABS(VTA.WN)*WA.WN : ' surface stalled?
7750
7820 POWER.WN = ABS(X.WN*VA(1))
7840 POWER = POWER.MR + POWER.TR + POWER.WN + HP.LOSS*550
7850
7860 ***** Vertical tail *****
7870
7880 Compute aerodynamic forces on vertical tail
7890
7895 VA.VT=VA(2)+VI.TR-D.VT*VA(6)
7897 VTA.VT=SQR(VA(1)*VA(1)+VA.VT*VA.VT)
7900 Y.VT=R2*(YUU.VT*ABS(VA(1))*VA(1) + YUV.VT*ABS(VA(1))*VA.VT)
7910
7940 IF ABS(VA.VT)>.3*ABS(VA(1)) THEN Y.VT=R2*YMAX.VT*ABS(VTA.VT)*VA.VT : ' surface stalled?
7970
8000 L.VT = Y.VT*H.VT
8010 N.VT = -Y.VT*D.VT
8020
8030 ***** General force equations *****
8040
8050 X.GRAV = -M*GRAV*S5 : ' gravity forces
8060 Y.GRAV = M*GRAV*S4*C5
8070 Z.GRAV = M*GRAV*C5*C4
8080
8090 |-----|
8100 | gravity | M.R. | FUS. | T.R | H.T. | WING | V.T. | component|
8110 |-----|
8120 |
8130 F(1) = X.GRAV + X.MR + X.FUS + X.WN : ' X-force |
8140 F(2) = Y.GRAV + Y.MR + Y.FUS + Y.TR + Y.VT : ' Y-force |
8150 F(3) = Z.GRAV + Z.MR + Z.FUS + Z.HT + Z.WN : ' Z-force |
8160 F(4) = + L.MR + L.FUS + L.TR + L.VT : ' L-moment|
8170 F(5) = + M.MR + M.FUS + M.HT : ' M-moment|
8180 F(6) = + N.MR + N.TR + N.VT : ' N-moment|
8190 |
8192 F(7) = GR(7)/ITB : pitch flap
8193 F(8) = GR(8)/ITB : roll flap
8200 |-----|
8210
8270 IF CHECK=0 THEN GOSUB 11040 : ' fill force component array
8290
8300 Body Accelerations
8310
8320 AB(1) = - (VB(5)*VB(3)-VB(6)*VB(2)) + F(1)/M
8330 AB(2) = (VB(4)*VB(3)-VB(1)*VB(6)) + F(2)/M
8340 AB(3) = (VB(1)*VB(5)-VB(4)*VB(2)) + F(3)/M
8350 AB(4) = F(4)/IX
8360 AB(5) = F(5)/IY - VB(4)*VB(6)*(IX-IZ)/IY + (VB(6)*VB(6)-VB(4)*VB(4))*IX/IY
8370 AB(6) = F(6)/IZ + IX*AB(4)/IZ
8380

```

```

8390 Integrate Body Accelerations
8400
8410 FOR IX = 1 TO 6
8420 VB(IX) = VB(IX) + ST * (A1 + AB(IX) + B1 + AP(IX))
8430 AP(IX) = AB(IX) : REM SAVE ACCEL PAST VALUES
8440 NEXT IX
8450
8470 Transform to earth (A/C rel to deck) velocities
8480
8490 VE(1) = (VB(1) + C5 + VB(3) + S5) + C4 + COS(XE(6))
8500 VE(2) = VB(2) + COS(XE(6)) + VB(1) + SIN(XE(6))
8510 VE(3) = (VB(1) + S5 - VB(3) + C5) + C4
8520 VE(4) = VB(4) + (VB(5) + S4 + VB(6) + C4) + TAN(XE(5))
8530 VE(5) = VB(5) + C4 - VB(6) + S4
8540 VE(6) = (VB(6) + C4 + VB(5) + S4) / C5
8550
8560 Integrate earth (A/C relative to deck) velocities
8570
8580 FOR IX = 1 TO 6
8590 XE(IX) = XE(IX) + ST * (A2 + VE(IX) + B2 + VP(IX))
8600 VP(IX) = VE(IX) : REM SAVE VEL PAST VALUES
8610 NEXT IX
8630
8640 TIME = TIME + ST
8650
8660 IF CHECK = 1 THEN IF CHECK.LOOP < CHECK.LOOP.MAX THEN GOTO 6020
8670 IF CHECK = 1 THEN GOSUB 12140
8680
8690 RETURN
8700

```

ORIGINAL PAGE IS
OF POOR QUALITY



Report Documentation Page

1. Report No. USA AVSCOM TR-87-A-7 NASA CR 177476		2. Government Accession No.		3. Recipient's Catalog No.	
4. Title and Subtitle Minimum-Complexity Helicopter Simulation Math Model			5. Report Date April 1988		
			6. Performing Organization Code		
7. Author(s) Robert K. Heffley Marc A. Mnich			8. Performing Organization Report No.		
			10. Work Unit No. 992-21-01		
9. Performing Organization Name and Address Manudyne Systems, Inc. 349 First Street Los Altos, California 94022			11. Contract or Grant No. NAS2-11665		
			13. Type of Report and Period Covered Final Contractor Report 7/85 to 7/87		
12. Sponsoring Agency Name and Address National Aeronautics and Space Administration, Washington, D.C. 20546-0001, and US Army Aviation Systems Command, St. Louis, MO 63120-1798			14. Sponsoring Agency Code		
			15. Supplementary Notes Point of Contact: Michelle M. Eshow (Contract Technical Monitor) Aeroflightdynamics Directorate M/S 211-2, Ames Research Center, Moffett Field, CA 94035 (415) 694-5272 FTS 464-5272		
16. Abstract <p>An example of a minimal complexity simulation helicopter math model is presented. Motivating factors are the computational delays, cost, and inflexibility of the very sophisticated math models now in common use. A helicopter model form is given which addresses each of these factors and provides better engineering understanding of the specific handling qualities features which are apparent to the simulator pilot. The technical approach begins with specification of features which are to be modeled followed by a build-up of individual vehicle components and definition of equations. Model matching and estimation procedures are given which enable the modeling of specific helicopters from basic data sources such as flight manuals. Checkout procedures are given which provide for total model validation. A number of possible model extensions and refinements are discussed. Math model computer programs are defined and listed.</p>					
17. Key Words (Suggested by Author(s)) helicopter, helicopter simulation, mathematical modeling, real-time simulation, handling qualities, helicopter dynamics			18. Distribution Statement Unclassified-Unlimited Subject Category 08		
19. Security Classif. (of this report) Unclassified		20. Security Classif. (of this page) Unclassified		21. No. of pages 100	22. Price